NAVAL POSTGRADUATE SCHOOL

MONTEREY, CALIFORNIA

THESIS

SIMULATION OF THE ACOUSTIC PULSE EXPECTED FROM THE INTERACTION OF ULTRA-HIGH ENERGY NEUTRINOS AND SEAWATER

by

Michael Gruell

March 2006

Thesis Advisor: Daphne Kapolka

Approved for public release; distribution is unlimited.

THIS PAGE INTENTIONALLY LEFT BLANK

REPORT DOCUMENTATION PAGE	*Form Approved OMB No. 0704-0188*

1. AGENCY USE ONLY (*Leave blank*)	**2. REPORT DATE** March 2006	**3. REPORT TYPE AND DATES COVERED** Master's Thesis	
4. TITLE AND SUBTITLE: Title (Mix case letters) Simulation of the Acoustic Pulse Expected from the Interaction of Ultra-High Energy Neutrinos and Seawater			**5. FUNDING NUMBERS** N/A
6. AUTHOR(S) Michael Gruell			
7. PERFORMING ORGANIZATION NAME(S) AND ADDRESS(ES) Naval Postgraduate School Monterey, CA 93943-5000			**8. PERFORMING ORGANIZATION REPORT NUMBER**
9. SPONSORING /MONITORING AGENCY NAME(S) AND ADDRESS(ES) N/A			**10. SPONSORING/MONITORING AGENCY REPORT NUMBER**
11. SUPPLEMENTARY NOTES The views expressed in this thesis are those of the author and do not reflect the official policy or position of the Department of Defense or the U.S. Government.			
12a. DISTRIBUTION / AVAILABILITY STATEMENT Approved for public release; distribution is unlimited.			**12b. DISTRIBUTION CODE** A

13. ABSTRACT (maximum 200 words)

The purpose of this thesis was to design, build, and test a device capable of simulating the acoustic pulse expected from the interaction between an Ultra-High Energy (UHE) neutrino and seawater. When a neutrino interacts with seawater, the reaction creates a long, narrow shower of sub-atomic particles. The energy from this reaction causes nearly instantaneous heating of the seawater on an acoustic timescale. The acoustic pulse created by the resulting thermal expansion of the water is predicted to be bipolar in shape. This work was undertaken to support a Stanford experiment, the Study of Acoustic Ultra-high energy Neutrino Detection (SAUND), that uses existing hydrophone arrays to detect UHE neutrinos from the acoustic pulse generated by their rare interactions with seawater.

The device fabricated for this thesis uses the discharge current from a 4μF capacitor charged to 2.5kV to heat the seawater between two copper plates. The anode and cathode plates of this "zapper" design were 6 cm in diameter and 20 cm apart. The acoustic pulse generated by the zapper was measured both in a small test tank at NPS and at the Acoustic Test Facility located at NUWC Keyport. Bipolar pulses observed at NPS on two separate test dates had average pulse lengths of 110μs +/- 10μs and 160 +/- 20μs and average amplitudes at 1m of 1.9 +/- 0.3Pa and 4.7 +/- 0.6Pa. The average pulse length recorded at Keyport was 49 +/- 6μs and the average amplitude at 1m was 6.4 +/- 0.9Pa. The pulse lengths recorded at NPS were reasonably consistent with theory, however all pressure amplitudes were about 100 times lower than predicted. The cause of the amplitude discrepancy is not completely understood at this time.

14. SUBJECT TERMS Neutrino detection, neutrino acoustic signature, electric discharge through seawater			**15. NUMBER OF PAGES** 80
			16. PRICE CODE
17. SECURITY CLASSIFICATION OF REPORT Unclassified	**18. SECURITY CLASSIFICATION OF THIS PAGE** Unclassified	**19. SECURITY CLASSIFICATION OF ABSTRACT** Unclassified	**20. LIMITATION OF ABSTRACT** UL

THIS PAGE INTENTIONALLY LEFT BLANK

SIMULATION OF THE ACOUSTIC PULSE EXPECTED FROM THE INTERACTION OF ULTRA-HIGH ENERGY NEUTRINOS AND SEAWATER

Michael S. Gruell
Lieutenant, United States Navy
B.S., George Washington University, 1999

Submitted in partial fulfillment of the
requirements for the degree of

MASTER OF SCIENCE IN APPLIED PHYSICS

from the

NAVAL POSTGRADUATE SCHOOL
March 2006

Author: Michael Gruell

Approved by: Daphne Kapolka
                 Thesis Advisor

                 James Luscombe
                 Chairman, Department of Physics

THIS PAGE INTENTIONALLY LEFT BLANK

ABSTRACT

The purpose of this thesis was to design, build, and test a device capable of simulating the acoustic pulse expected from the interaction between an Ultra-High Energy (UHE) neutrino and seawater. When a neutrino interacts with seawater, the reaction creates a long, narrow shower of sub-atomic particles. The energy from this reaction causes nearly instantaneous heating of the seawater on an acoustic timescale. The acoustic pulse created by the resulting thermal expansion of the water is predicted to be bipolar in shape. This work was undertaken to support a Stanford experiment, the Study of Acoustic Ultra-high energy Neutrino Detection (SAUND), that uses existing hydrophone arrays to detect UHE neutrinos from the acoustic pulse generated by their rare interactions with seawater.

The device fabricated for this thesis uses the discharge current from a 4μF capacitor charged to 2.5kV to heat the seawater between two copper plates. The anode and cathode plates of this "zapper" design were 6 cm in diameter and 20 cm apart. The acoustic pulse generated by the zapper was measured both in a small test tank at NPS and at the Acoustic Test Facility located at NUWC Keyport. Bipolar pulses observed at NPS on two separate test dates had average pulse lengths of 110μs +/- 10μs and 160 +/- 20μs and average amplitudes at 1m of 1.9 +/- 0.3Pa and 4.7 +/- 0.6Pa. The average pulse length recorded at Keyport was 49 +/- 6μs and the average amplitude at 1m was 6.4 +/- 0.9Pa. The pulse lengths recorded at NPS were reasonably consistent with theory, however all pressure amplitudes were about 100 times lower than predicted. The cause of the amplitude discrepancy is not completely understood at this time.

THIS PAGE INTENTIONALLY LEFT BLANK

TABLE OF CONTENTS

THIS PAGE INTENTIONALLY LEFT BLANK

LIST OF FIGURES

THIS PAGE INTENTIONALLY LEFT BLANK

LIST OF TABLES

THIS PAGE INTENTIONALLY LEFT BLANK

ACKNOWLEDGMENTS

THIS PAGE INTENTIONALLY LEFT BLANK

I.   INTRODUCTION

The purpose of this thesis was to simulate the acoustic pulse created by the interaction between an Ultra-High Energy (UHE) neutrino and seawater. The interaction between a neutrino and seawater forms a shower of subatomic particles. The energy from this shower results in near instantaneous heating of the seawater. An acoustic pulse is formed from the resultant expansion of the seawater as it heats up. The pulse formed is expected to be a bipolar pulse that goes positive first. The pulse length and amplitude depend on the properties of the seawater in addition to the dimensions of the shower.

In 2001, Giorgio Gratta of Stanford University began an experiment to detect UHE neutrinos acoustically using a matched filter to detect the acoustic pulse received by existing hydrophone arrays. This project is referred to as the Study of Acoustic Ultra-high Neutrino Detection (SAUND) and is currently based on a large hydrophone array that the US Navy operates for naval exercises at the Atlantic Undersea Test and Evaluation Center (AUTEC).

In order to examine the possibility of detecting the acoustic pulse from a neutrino-seawater interaction, a decision was made in collaboration with Stanford to build a device to simulate the acoustic signature at AUTEC. This device, or "zapper", would test SAUND's ability to pick up the desired signal as well as to determine the ability of SAUND to correlate signals from different hydrophones. The zapper would be deployed underwater and attempt to simulate the neutrino's reaction by discharging a capacitor through the seawater.

The design of the zapper went through many iterations and a working prototype was constructed and tested in January 2006. The zapper prototype was tested twice in a saltwater tank at the Naval Postgraduate School (NPS) and then tested underwater at the Acoustic Test Facility (ATF) at the Naval Undersea Warfare Center (NUWC) located in Keyport, WA. Initial testing revealed the expected bipolar pulse. The pulse durations measured at NPS were in reasonable agreement with established theory, however, all amplitudes were two orders of magnitude lower than anticipated.

THIS PAGE INTENTIONALLY LEFT BLANK

II.   BACKGROUND

A.   NEUTRINO INTERACTIONS WITH SEA WATER

A neutrino with an energy greater than 10^{18} eV is considered to be UHE. Cosmic rays from beyond our galaxy are one source of these UHE neutrinos. When a neutrino reacts with a water molecule, it creates a hadronic shower. Dolgoshien and Askaryan first proposed in 1957 that a high-energy charged particle in water would create a thermal shock resulting in the emission of an acoustic pulse. According to Lehtinen et. al. [2002], the particle shower created by the reaction is elongated into a long, thin vertical column approximately 20m long. The mechanism that creates the acoustic pulse is the near instantaneous heating of the water in the vertical column of the shower. The resultant pulse is created by the summation of the expansion of infinitesimal volumes in the column.

Assuming that the energy deposition can be expressed in terms of a delta function in both space and time, Learned [1979] solves for the pressure as a function of distance and time as:

Eq 1 $$p(r,t) = \frac{E_o K}{4\pi C_p} \frac{\delta'(r/c - t)}{r},$$

where K is the thermal expansion coefficient, C_p is the specific heat, E_o is the total energy deposited and c is the speed of sound. Using the more realistic Gaussian heat distribution, the equation becomes:

Eq 2 $$p(r,t') = -\frac{E_o K}{4\pi C_p} \frac{t'}{\sqrt{(2\pi)}(\sigma/c)^3} \exp[-(t')^2/2(\sigma/c)^2],$$

where t' is the retarded time, $t - r/c$, and σ is the standard deviation of the heat deposition in time. This is a bipolar pulse which swings positive first. An example of the expected pulse is shown in Figure 1.
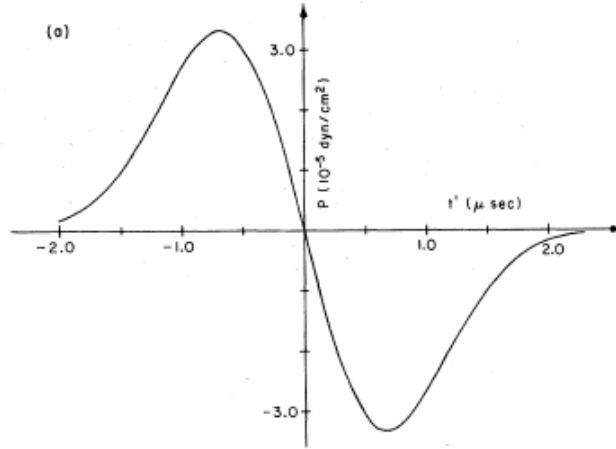
Figure 1.   Calculated acoustic pulse from neutrino interactions. From Learned [1979]

The pressure amplitude is calculated assuming that the shower column is uniformly heated and the length is much larger than the diameter. This equation is given by Sulak et. al. [1979] as:

Eq 3 $P \cong \dfrac{K}{C_p} \dfrac{E_o}{r} \dfrac{c^2}{8d^2} \dfrac{\sin x}{x}$,

Where $x = \left(\dfrac{\pi L}{\lambda}\right)\sin\theta$, L is the length of the column, and d is the diameter of the column, and θ is the angle to the measurement point relative to the acoustic axis. The pulse length is dependent on the geometry of the shower's vertical column as well as the time period over which the energy is deposited. It is calculated as the summation of the time period over which the energy is deposited plus twice the time that it takes sound to travel from one side of the column to the other.

B.   STUDY OF ACOUSTIC HIGH-ENERGY NEUTRINO DETECTION (SAUND)

During the 1970's, the Deep Underwater Muon And Neutrino Detection (DUMAND) project was designed to detect UHE neutrinos from Čerenkov radiation. Although acoustic detection was considered, it was not accomplished before the project was discontinued in 1996. The idea of the acoustic detection of neutrinos was resurrected around 2001 and is being pursued by a number of groups. Giorgio Gratta of the Stanford High Energy Physics group has established the Study of Acoustic Ultra-high energy

4

Neutrino Detection (SAUND) to use pre-existing hydrophone arrays to detect neutrinos acoustically. The hydrophone arrays currently being used are the new AUTEC Hydrophone Replacement Program (AHRP) arrays located in the Tongue of the Ocean in the Bahamas. These bottom mounted hydrophone arrays are approximately 2km in depth and cover an area of approximately $250\,km^2$. A conceptual picture of an AHRP hydrophone detecting the acoustic pulse from a hadronic shower is shown in Figure 2.
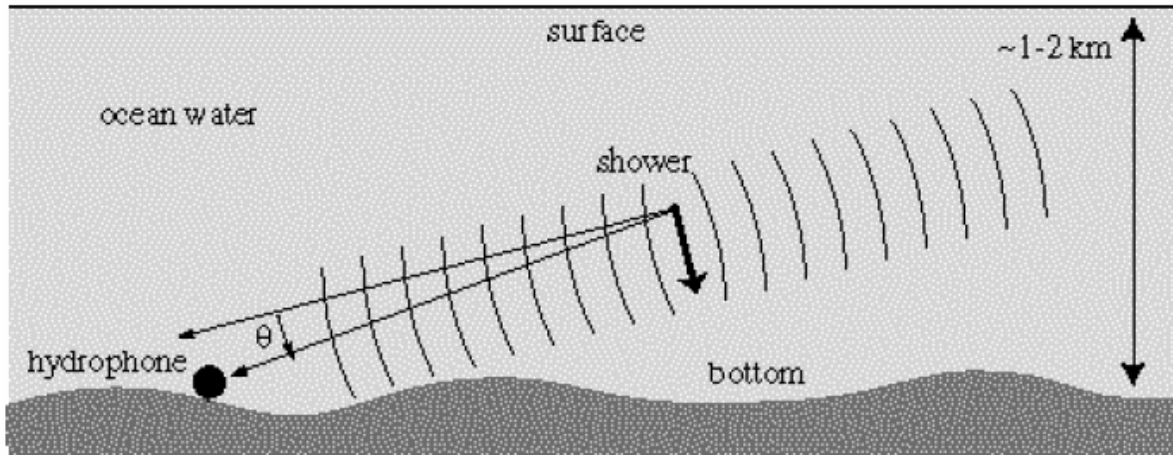
Figure 2.   Example of acoustic detection of pulse created from hadronic shower. From Lehtinen et. al. [2002]

SAUND computers receive the raw hydrophone data from the AHRP arrays. A master computer controls the timing and the noise thresholds that are applied to the data. A matched filter using the bipolar pulse shown in Figure 1 attempts to detect the rarely occurring neutrino signature amidst the voluminous data acquired.

Due to uncertainties in both how the AUTEC environment and the AHRP electronics would affect the neutrino's acoustic signature, a calibration was proposed to characterize the AHRP system. In addition, it was necessary to ensure that the signal expected from a UHE neutrino could in fact be detected by the AHRP hydrophones. The calibration required designing and building a device which could mimic the acoustic pulse described in Chapter II by using an electric discharge to quickly heat the water in a column of seawater. Since this device would in effect "zap" the water with electricity, this device was dubbed the "zapper".

THIS PAGE INTENTIONALLY LEFT BLANK

III.   DESIGN

A.   INITIAL DESIGN

As described in the previous chapter, the goal of the zapper was to simulate the acoustic signature expected from the reaction between a neutrino and seawater. Because of the expected length of the hadronic shower, the initial zapper design involved discharging a capacitor through seawater between an anode and a cathode placed 10m apart from each other. To contain the path of the resulting current to a small cross-sectional area, the design called for a 2 cm diameter helical strip of plastic insulation to be wrapped around the axis from the anode to the cathode. A rough initial sketch of this design is shown in Figure 3.   In order to verify the expected acoustic signature which would be detected by the AUTEC hydrophones from neutrino interactions at various depths and from various directions, preliminary designs called for having the "zapper" discharge periodically while spiraling down through the water column. Since the water depth near the AUTEC AHARP arrays extends to 1.6km, the pressure vessel for the supporting electronics had to have a depth tolerance of about 160atm. The plans also included a float and detachable anchor to recover the device after its descent.
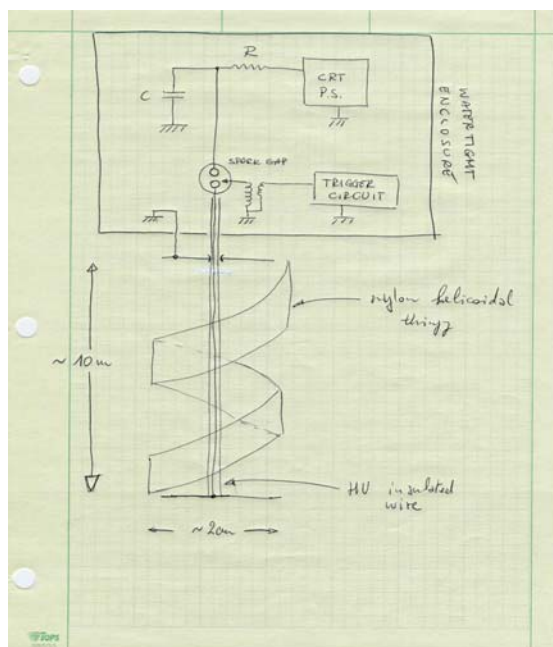

Figure 3.   Sketch for zapper original design. From Gratta [2005]

The electronics portion of this initial design called for a capacitor to hold and discharge the electricity. The seawater serves as the load, and a spark gap switch controls the capacitor discharge. The initial design also called for a pressure sensor to "turn on" the zapper at a depth of 30m. A trigger circuit was envisioned as a means to turn the spark gap switch on periodically after the capacitor was fully charged.. To mimic the neutrino signature, the energy to be discharged was 1J or about 10^{19} eV. The resistance of the water column between the anode and cathode can be found using the equation:

$$\textbf{Eq 4}\ \ R = \frac{L}{A}\rho\ ,$$

where L is the length of the cylinder of water between the anode and cathode, A is the cross-sectional area, and ρ is the resistivity of sea water. Using the accepted value of 0.2 $\Omega - m$ as the resistivity of seawater (Boyd [2006]), and inserting the values for L (10m) and A ($\pi (1\ cm)^2$), the resistance of the cylinder of seawater is calculated to be $6.4\,k\Omega$. To create the thermal heating on a sufficiently small time scale, the time constant for the discharge was set at $5\,\mu s$. Using the relationship between the discharge time constant, the capacitance, and the resistance:

$$\textbf{Eq 5}\ \ C = \frac{\tau}{R},$$

the desired capacitor value is found to be 833pF. This value was rounded up to 1nF to get a standard value. The voltage needed to dump 1J of energy into the water is then found using the equation:

$$\textbf{Eq 6}\ \ V = \sqrt{\frac{2E}{C}}\ ,$$

where E is total energy. This resulted in a voltage of 45 kV. Unfortunately, this value was too high for the available high voltage components as the highest value of spark gap switch readily available was rated at 30kV. Because higher voltages require larger capacitors to avoid dielectric breakdown, 45kV also drove the design to a larger capacitor which would, in turn, require a larger pressure vessel.. By doubling the capacitance to 2nF, the voltage required could be dropped to 30kV enabling the use of smaller and more readily available components. The higher capacitance doubled the time constant from

$5\,\mu s$ to $10\,\mu s$. While any increase in the pulse length is undesirable from the point of view of simulating the near instantaneous heating of seawater due to a neutrino interaction, the trade-off was deemed acceptable since the simulated pulse – although longer – could still be used to validate the ability of SAUND II to detect neutrino-like acoustic signatures.

B. REFINING THE INITIAL DESIGN

With the assistance of Don Snyder, a technician in the Rail Gun Group at NPS, a rudimentary desktop model was constructed to test the electronic design. A schematic of this design is shown on Figure 4, and a picture of the desktop model is shown on Figure 5. Four mica 500pF capacitors were put in parallel to provide the 2nF of capacitance. The power source was a variable 0-30kV DC voltage supply. The spark gap switch chosen was a gas-filled switch using sulfur hexafluoride. This was chosen as it was readily available and could withstand at least 30kV.
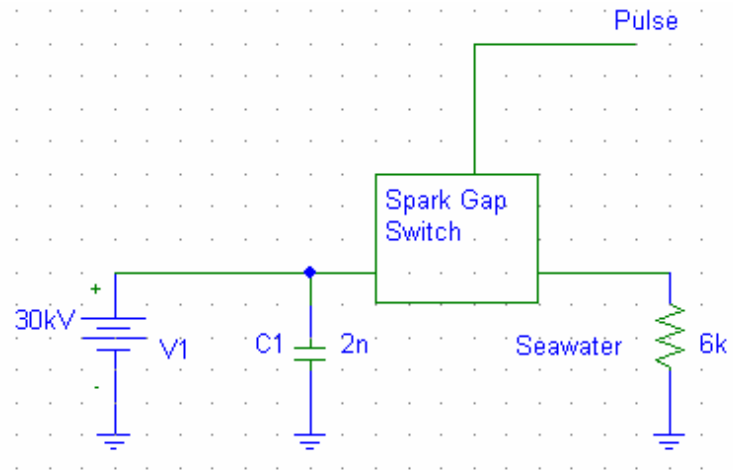
Figure 4.   Schematic of zapper initial design

The desktop model provided many lessons towards making a working prototype. One challenge was that the gas spark gap switch was unreliable. During testing, it would discharge the capacitor about half the time. This was attributed to the fact that the particular spark gap switch that was being used was made to work at 50kV, and 30kV was towards the bottom of its operating range. Another challenge while working with this design was the difficulty in measuring data. Many commercial devices such as an

oscilloscope or a voltmeter could not function at 30kV. The solution was to use a commercial voltage divider to track the charging of the zapper, and a Pearson current monitor to indirectly measure the current as the capacitor discharged. The final significant challenge that was observed was the need to place components at least an inch from each other. This is due to the fact that dielectric breakdown of air occurs at approximately 25kV per inch. Since the components need to be in close proximity in the pressure vessel, this limitation posed a challenge for the prototype. A possible solution might be to cover the components in an insulating material at the final construction.
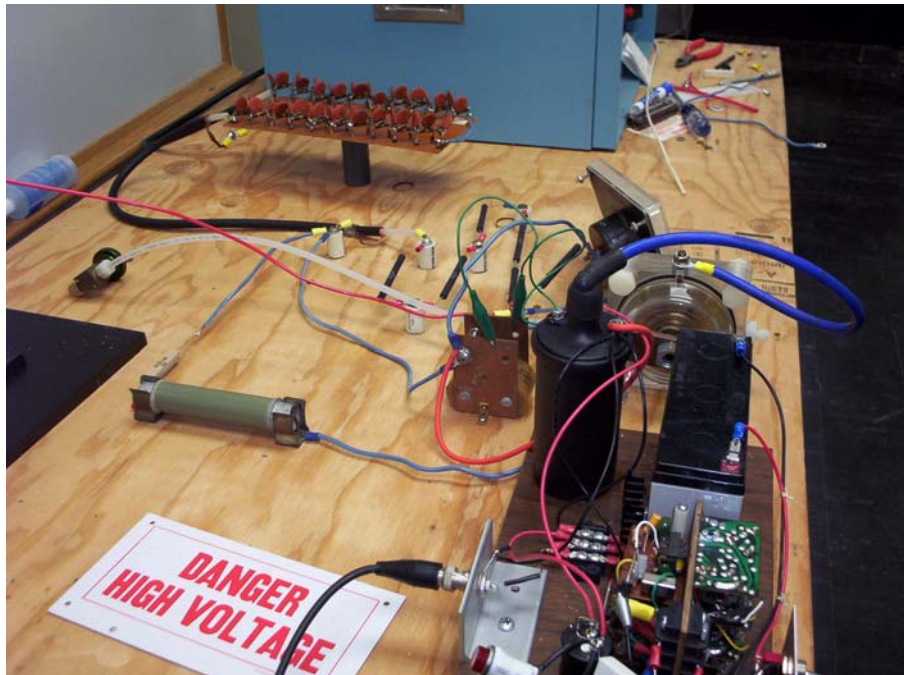
Figure 5.   Desktop model of initial design

After consulting with the Stanford High Energy Physics (HEP) group, a decision was made to scale back the design of the zapper to create a simpler version for the first stage of testing. One of the main concerns was to "shrink" the conducting path to a more manageable size for fabrication and testing purposes. The dimensions chosen were a length of 20cm and a diameter of 10cm. This shorter length was also expected to produce the additional advantage of a more omni-directional pulse. Another way in which the design was simplified was by removing the requirement for continuous operation during its descent to the bottom. Instead, the simplified version was envisioned as operating while suspended from a boat. Its depth was intended to be sufficiently far

beneath the surface to avoid having surface reflections interfere with the pulse received from the direct path. Given the shorter length and larger diameter of the new design, the conducting cylinder's resistance was expected to decrease from $6\,k\Omega$ to $5\,\Omega$ using Eq 4. Also, in order to increase the likelihood of detecting the acoustic signal, the total energy to be released into the water was increased from 1J to at least 10J. For the purpose of using readily available parts, a $4\,\mu F$ capacitor was chosen, and the voltage was raised slightly to 2.5kV (the upper limit of the capacitor.) At this voltage there are alternatives to a spark gap switch such as high power transistors. At 2.5kV, the $4\,\mu F$ capacitor delivers 12.5J of energy to the seawater with a time constant of $20\,\mu s$. The parameters chosen for the simplified zapper design were therefore:

- $C = 4\mu F$
- $V = 2.5$kV
- $L = 20$cm
- $d = 10$cm

C. FINAL DESIGN

1. Selecting the Main Components

As noted above, the decision to lower the voltage made acquiring parts easier, however, the components still need to tolerate fairly high currents. This made finding a suitable switching mechanism challenging. The expected peak current was calculated to be 490A. The original plan was to use a vacuum spark gap for the switching mechanism. However, there was a minimum wait of four weeks for that part so a replacement part was sought. After consulting with Professor Alex Julian of the Electrical Engineering Department at NPS, a suitable alternative was identified, an Insulated Gate Bipolar Junction Transistor (IGBT). The IGBT chosen was a Powerex CM400-90H rated at 4.5kV and 400A. Typical commercial uses would be switching applications where high switching speed and high power were needed, such as in subways. The selection of the IGBT necessitated small changes to the circuit design. To protect the IGBT it was placed between the load and ground instead of between the capacitor and the load as was initially intended. This change is illustrated in Figure 6.
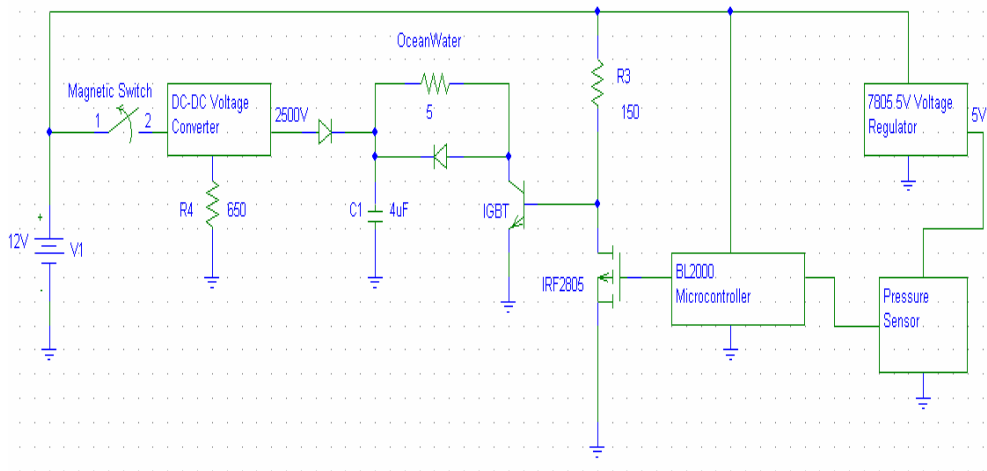
11

Figure 6.　　Schematic of zapper final design

The power was supplied by a 12V battery. The type of battery chosen was a 7.5 Amp hour Solid Lead Acid (SLA) battery. The SLA battery was chosen because of its relatively high energy density, its availability, and its reliability. 12V was chosen because it could power most types of anticipated circuitry and is the voltage required by most types of commercial DC-DC voltage converters. A DC-DC voltage converter was chosen to amplify the 12V to the required 2.5kV. The voltage converter chosen was an EMCO DX100, which is a variable 1.5-10kV converter. It has three inputs, a ground, an input for 12V, and a third input that controls the voltage output by acting as a potentiometer. Through testing, it was found that a $650\,\Omega$ resistor between the third input and ground provided the required 2.5kV output.

The circuit requires two diodes to provide protection. One diode is connected to the output of the DC-DC voltage converter. This is done to prevent potentially damaging feedback to the voltage converter. The second diode is placed between the capacitor and the collector of the IGBT. This is done to provide an alternative path for the current in case the IGBT unexpectedly turns off. These diodes are shown in Figure 6.

A magnetic proximity switch is placed in series with the 12V battery and the power lead of the DC-DC converter as shown in Figure 6. This provides a mechanical safety for the zapper. The magnetic switch has options for both normally open and normally closed (with no magnet applied). The option chosen for the zapper was to use the normally open option. In this configuration no power goes to the DC-DC voltage

12

converter unless the magnet is applied. Once the magnet is applied, the battery powers the voltage converter, and the capacitor starts to charge. The magnetic switch is affixed to the inside of the pressure vessel. When ready to commence charging the capacitor, the magnet is attached to the outside of the pressure vessel directly over the switch. A magnet strong enough to activate the switch through the pressure vessel wall was found from an old 3.5" floppy drive. This arrangement provides another type of safety measure as well. When the magnet is detached from the outside of the pressure vessel, the capacitor can no longer be charged up. However, it can still have a residual charge. Since the power to the rest of the circuit is still on, the triggering mechanism remains active. Therefore, the zapper will discharge any remaining charge on the capacitor after a short wait and is then safe to retrieve from the water. And finally, for the $4uF$ capacitor, a doorknob mica capacitor was chosen both for its availability, its size (9cm diameter, 5 cm thick), and its low inductance ($\sim 20 \mu H$).

2.   Trigger Circuit and Pressure Sensor

Originally it was thought that the DC-DC power converter needed a resistor in series to limit the current to 5mA. The value of the charging resistor needed was determined to be approximately $1 M\Omega$. This value results in a time constant of four seconds for charging the capacitor. The discharge time constant was determined to be $20 \mu s$.   Thus, a pulse was needed to "turn on" the IGBT for 200ms and "turn off" the IGBT for four seconds. The off time was extended to five seconds to add a buffer to allow the capacitor to charge fully. After reviewing the spec sheet and testing the IGBT, the voltage required to turn on the IGBT was 6V, and the current required was approximately 50mA. Preliminary attempts to accomplish this with an LM555 timer integrated circuit (IC) chip were unsuccessful due to the low duty cycle, so the next step was to try two LM555's in parallel. This attempt was also unsuccessful. Although the use of a microprocessor had initially been rejected as too space consuming, it presented itself at this point as the only option. The microprocessor chosen was a Z-World BL2000. This microprocessor was already available and had the advantage of being familiar. It uses the Dynamic C programming language which is very similar to C. Producing the pulse with the BL2000 proved to be quite simple. The BL2000 was

programmed to output a TTL "high" (5V), wait for 200ms, output a TTL "low" signal (0V), and wait for 5000ms (five seconds) while in an infinite loop.

As it turned out, the program had to be modified slightly due to the DC-DC voltage converter. The converter could only output a maximum current of $100\,\mu A$. After reviewing the specs and noting that the voltage converter had short circuit protection, the charging resistor was removed. Testing the charge time without the charging resistor, the capacitor required two minutes to become fully charged.

```
//Zapperpulse.c ---creates pulse for zapping


void main()
{
int ms;          //number of milliseconds to wai
int comp;        //input from comparator
long t0;
float volt;




brdInit();


    while (1)
    {
        digOut(3,1);
        for (t0=MS_TIMER; MS_TIMER<t0+120000;);
        digOut(3,0);
        for (t0=MS_TIMER; MS_TIMER<t0+200;);
    }
}
```

Figure 7.   Dynamic C program used in BL200 microcontroller

The output of the microprocessor alone can't turn on the IGBT, so a small amplifier circuit is needed. A HEXFET IRF 2805 in the common source mode is used to amplify the signal as shown in Figure 6. When the BL2000 outputs 0V, the output of the amplifier is 12V, and when the output of the BL2000 is 5V, the amplifier outputs 0V. Thus, the pulse is inverted. The program of the BL2000 was adjusted to compensate for this. The output going into the gate of the IGBT is a 12V pulse for 200ms followed by 0V for two minutes. The final program is shown in Figure 7.

To turn the zapper on at the desired depth, the Measurement Specialties MSP 600-100-P-3-D-4 pressure sensor was chosen to provide a voltage signal which could be fed to the microcontroller to control the charging process. The pressure sensor requires 5V

14

for power, so a 7805 5V voltage regulator is used to draw down the 12V from the battery to 5V. Tests of the pressure sensor revealed that it read 0.53V at ambient pressure and increased at a rate of approximately 0.01V per 10cm in fresh water. To turn the zapper on at a depth of about half a meter, therefore, would require the microcontroller to activate the charging process with an input signal of 0.6V. To accomplish this with the microcontroller, the pressure sensor output was connected to one of the inputs of the microcontroller, and the program was adjusted to output the pulse when the input is greater than 0.6V. If the voltage falls below 0.6V, the microcontroller stops. Using Dynamic C, this was accomplished by using an "IF..ELSE" statement and is shown in Figure 8.

```
//Zapperpulse.c ---creates pulse for zapping


void main()
{
int ms;          //number of milliseconds to wai
int comp;        //input from comparator
long t0;
float volt;




brdInit();


    while (1)
    {
        volt = AnaInVolt(7);
        if (volt > 0.6)
        {
        digOut(3,1);
        for (t0=MS_TIMER; MS_TIMER<t0+120000;);
        digOut(3,0);
        for (t0=MS_TIMER; MS_TIMER<t0+200;);
        volt = AnaInVolt(7);
        }
        else{
        digOut(3,1);
        }
        AnaInVolt(7);
    }
}
```

Figure 8.   Dynamic C program incorporating pressure sensor

3.   Pressure Vessel

In order to protect electronics at depth, a pressure vessel is required. Commercial pressure vessels require long lead times and are quite expensive. As an alternative, a pressure vessel manufactured by the Oceanography Department at NPS was chosen. This

pressure vessel was cheaper than commercial pressure vessels. In addition, the short lead time of one week allowed for sufficient time to determine the exact size specifications needed to accommodate the electronic components that were to be housed inside.

Once all the parts were in hand, the size of the pressure vessel was determined to be 3ft long and 8in in diameter (inner). A 5in wide aluminum tray was fitted inside the pressure vessel to mount the electronics. A sheet of 1/4 inch thick PVC was placed over the aluminum tray to provide a insulated base for the zapper. The pressure vessel has 3 openings to the water. Two are on one end of the vessel to accommodate the conducting cables carrying the discharge current. The third opening is on the other end of the pressure vessel where the pressure sensor fits.

4. Conducting Channel

The conducting channel consists of two conducting plates 6cm in diameter and set 20cm apart. The plates are made of copper since it was readily available and is an excellent conductor. Testing was done to ensure that corrosion would not affect the results during the duration of the experiments, and the result of these tests are detailed in the "Testing" section. To prevent possible fringing of the discharge current, the design called for insulation around the conducting path between the plates. Towed array tubing was chosen because it is designed to match the impedance of seawater. The largest towed array tubing available, however, had an 8cm diameter. The support structure within the tube (required to hold and space the copper plates) reduced the space available for the plates even further. Therefore, the plates which were originally intended to be 10cm ended up as 6cm in diameter. The support structure consists of two plastic wheels with three rods connecting them. The copper plates are attached to the inside of the 8cm diameter wheels. The towed array tubing slides over this assembly. A sketch of the complete assembly of the conducting path is shown in Figure 9.
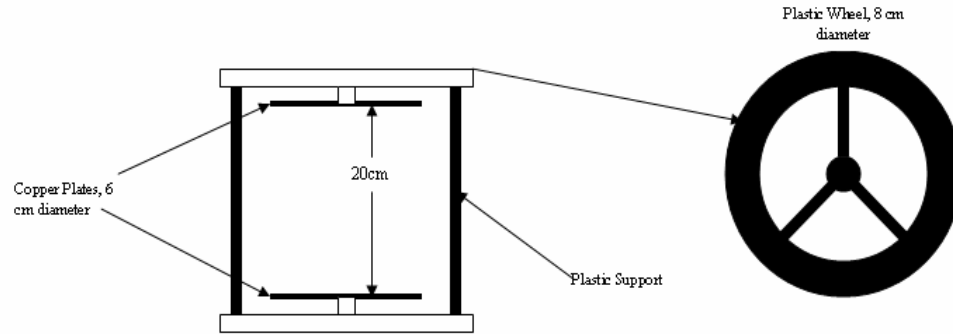
16

Figure 9.   Sketch of conduction path

The conducting path is rigidly fixed to the pressure vessel so that it remains vertical as the pressure vessel is lowered into the water. This is accomplished by using a semi-circular plastic piece attached to a 1.75cm (3/4 inch) PVC pipe that attaches to the conducting path.   The PVC pipe is 45cm long so as to minimize the scattering and reflection of the acoustic pulse off of the pressure vessel. The cables from the pressure vessel are affixed to opposite sides of the conducting path as shown on Figure 10.

Figure 10.   Conducting path with cables attached

THIS PAGE INTENTIONALLY LEFT BLANK

IV.   FABRICATION

A.   ELECTRICAL COMPONENTS

The manufacturing of the pressure vessel took approximately 14 days. The delay in the expected time was due to a wait for cable connectors. When the pressure vessel was ready, the electrical components were mounted on the aluminum tray.   The aluminum tray was five inches across and nearly three feet long, almost as long as the pressure vessel itself. To mount the electrical components, a sheet of PVC 1/4 inch thick was mounted on top of the aluminum tray to give the zapper an insulated surface. The PVC sheet was thick enough so the mounting screws of the components did not penetrate the PVC and contact the aluminum below.

The primary consideration for where to place the electrical components was the desire to minimize any Electromagnetic Interference (EMI) which might result from the large current occurring during discharge. EMI can adversely affect logic components such as the BL2000, 5V voltage regulator, and amplifier circuit. So, the capacitor was placed at the end of the vessel near the feedthroughs, and the logic components were located at the other end. Most of the components were four-five inches in dimension, so the components were mounted in a line.   Another goal in the placement of the components was to make the wiring between everything as short as possible.

Starting from the end opposite the feedthrough cables, the 12V battery was mounted first. The battery was mounted using a metal bracket that nearly encased the battery, leaving the terminals exposed. Figure 11 shows a picture of the mounted battery. The battery was placed here, because the BL2000 and logic circuits also needed to be placed at this end and required the 12V source. The next component mounted was the BL2000. The BL2000 had holes for mounting, so the BL2000 was screwed into place. The amplifier circuit, voltage regulator circuit and $650\,\Omega$ resistor for the DC-DC voltage regulator were soldered onto a prototype board. The power from the battery was also inserted into the prototype board to provide a central place for power for the zapper. The magnetic switch was placed in series between the 12V power and the power lead for the DC-DC voltage converter on the prototype board.   The prototype board was then

mounted onto plastic supports that were screwed into the BL2000. Figure 12 shows the prototype board mounted onto the BL2000 with the protective cover.   The pressure sensor was screwed into the pressure vessel's end cap on the battery's side. The photo of this is shown in Figure 13.
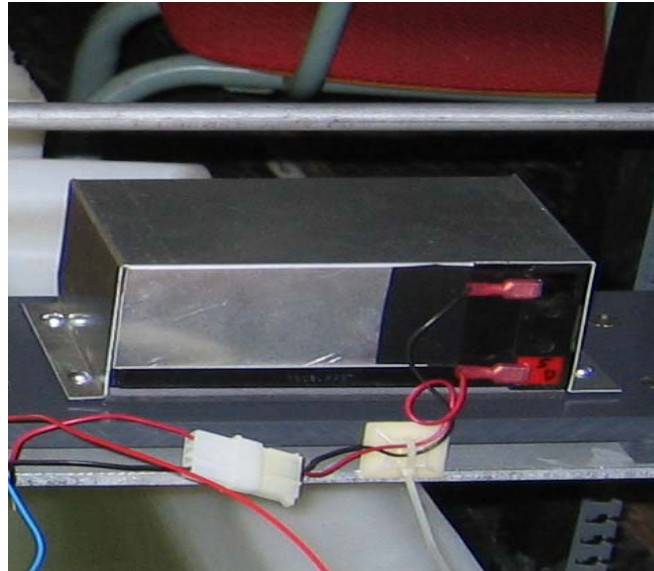

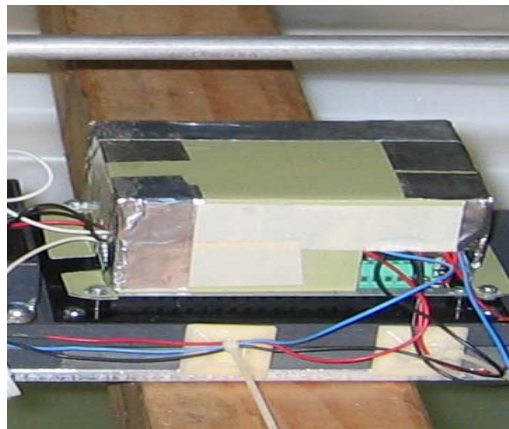Figure 11.   12V solid lead acid battery with mount

Figure 12.   PC board and BL2000 with protective cover

Figure 13.   Pressure sensor and end cap

The next part mounted was the IGBT since the inputs for the IGBT come from the prototype board. The DC-DC voltage converter was mounted next to the IGBT with a bracket. The IGBT and DC-DC voltage converter are shown mounted in Figure 14. Finally the capacitor was mounted at the far end of the device as close as possible to the feedthrough cables. The feedthrough cables on the inside of the zapper were too long, and these were cut and spliced with a smaller gauge wire to be connected to the capacitor. The capacitor was first put in a cradle, and then a bracket was placed around the capacitor and cradle. The mounted capacitor and the spliced inside cables are shown in Figure 15.
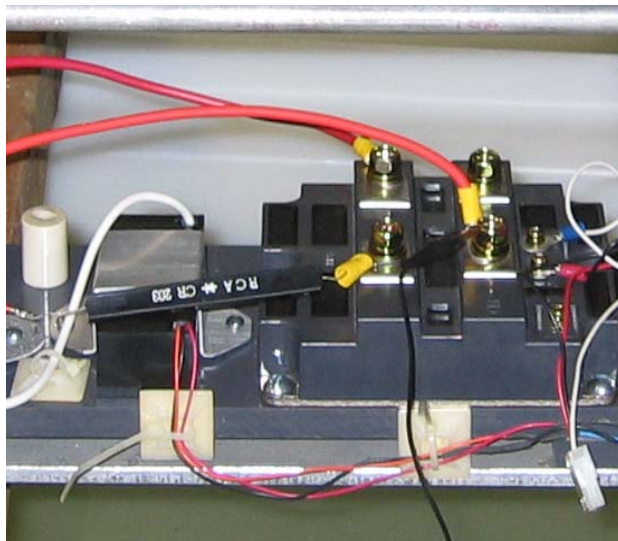

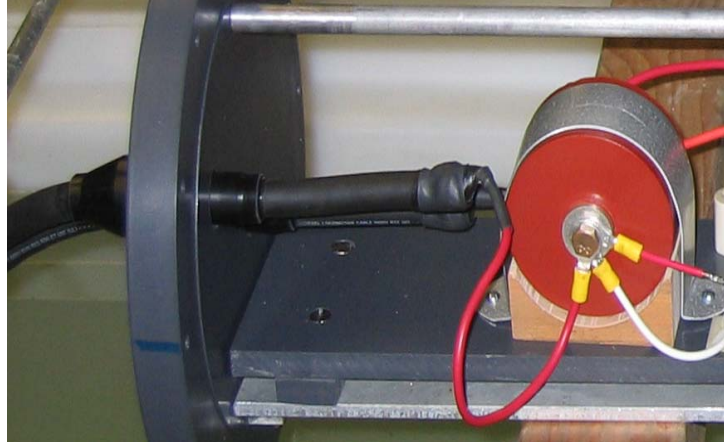Figure 14.   IGBT and DC-DC voltage converter

Figure 15.   4 μF capacitor

B.   PRESSURE VESSEL AND EXTERNAL COMPONENTS

The conducting path was originally constructed with the three ½ inch plastic supports shown in Figure 9. However, to minimize interference with the acoustic pulse, the plastic supports were decreased to 1/4". The conducting path without the towed array tubing attached is shown in Figure 16. The towed array cable was then slid over the conducting path. The towed array tubing arrived flattened and was therefore hard to put around the conducting path without damaging it. Heating the tubing made it more pliable. After fitting it on the conducting path, the tubing was slightly loose. A plastic screw was used to keep it in place. Figure 17 shows the conducting path with the towed array tubing on.

Figure 16.   Conducting path

22

Figure 17.   Conducting path with towed array tubing

The current carrying cables running through the feedthroughs were 0 gauge and had a voltage rating of 30kV Since these cables were extremely stiff and the voltage rating was higher than necessary for such a short pulse, the cables were reduced to a more manageable gauge (8). A 3M splice kit for underwater use was used to splice smaller cable to both ends. A molding was placed around the joint, and resin was poured into the molding and left to cure for 24 hours. Figure 18 shows the entire conducting path mounted and connected to the zapper.

Figure 18.   Zapper in pressure vessel with conducting path attached

THIS PAGE INTENTIONALLY LEFT BLANK

V.   TESTING

A.   NPS TESTS

1.   Initial Test

The initial test for the zapper was at NPS on January 17, 2006, in a polypropylene tank approximately 36cm x 72cm x 60cm (width, length, depth). The tank was filled to 55cm with fresh water from the sink in the laboratory. True seawater was not readily available in the quantity needed, so seawater was simulated by using sodium chloride water softener salt to approximate the salinity of seawater, 35ppt. Based on the volume of water in the tank, the amount of water softener salt needed was 80lbs. This was added to the tank and allowed to dissolve for 24 hours.

The purpose of this test was to test the zapper to see if the device was working as intended and to observe the nature of the acoustic pulse emitted to see if the pulse was as expected. For this test, the electronics portion of the zapper was positioned outside the polypropylene tank with the conducting path hanging in the water. Two four-by-four wooden planks were laid over the tank, and the zapper was suspended on them. The conducting path was held vertical in the center of the tank, and the midpoint was lowered to 28cm in depth. A Brüel and Kjær 8103 type hydrophone was initially 27cm away from the conducting path and held vertical with ring stands. Figure 19 shows a photo of this layout.

Figure 19.   NPS tank test

The battery to the zapper was connected and a magnet was applied to the magnetic switch to close the circuit between the DC-DC converter and the 12V battery to charge the capacitor. The capacitor was monitored using a DC probe rated at 6kV which lowered the voltage by a ratio of 1,000:1. This allowed the voltage across the capacitor to be read by a voltmeter. The circuitry of the zapper worked as designed.

An acoustic pulse was measured by the hydrophone and an example of this waveform can be seen in Figure 20. The sensitivity of the hydrophone was 26 $\mu V / Pa$ over the frequency range of the pulse. As expected, the waveform was observed to be bipolar; however, it appeared to go negative first. The hydrophone's position was varied 20-60cm in distance from the conducting path and was raised up to 10cm vertically from the midpoint of the conducting path. 22 waveforms were recorded during the testing. A table with the raw numerical data from the pulses which agreed with the expected bipolar pulse shape is shown on Table 1.

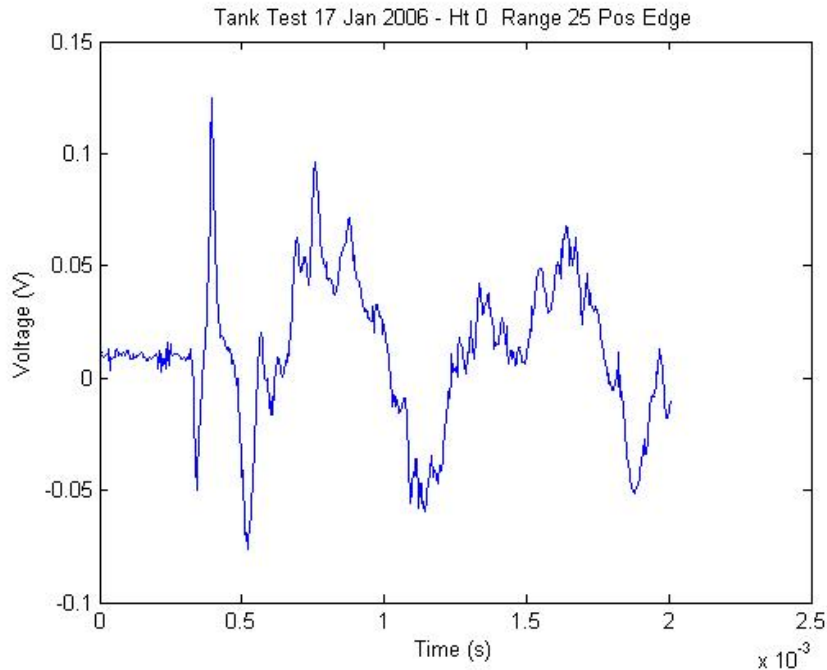| TEST #	Voltage (V)	Pressure (Pa)	Height (m)	Distance (m)	Pressure at 1m (Pa)	Pulse Length (us)
Test 7	0.083	6.38	even	0.2	1.28	130
Test 8	0.125	9.62	even	0.25	2.40	108
Test 15	0.082	6.31	even	0.3	1.89	95
Test 16	0.087	6.69	even	0.3	2.01	95
Test 17	0.088	6.77	even	0.3	2.03	110
Test 18	0.123	9.46	even	0.2	1.89	105
Test 19	0.125	9.62	even	0.2	1.92	105

Table 1.   Jan 17 Test Results

Figure 20.   Jan 17 NPS tank test zapper pulse

2.   Follow on tests

The zapper was tested in the tank again on January 25, 2006. The purpose of this test was to observe the acoustic pulse as well as the current levels using a Pearson Current Monitor Model 4997 which converted the current into voltage at a ratio of 100:1. The peak value of the current allowed a calculation of the resistance of the conducting path. This was used to calculate the effective resistivity of the saltwater tank assuming that the resistance of the cables could be neglected. The same experimental setup as the previous test was used. This time the hydrophone was kept at a constant distance of 27cm and the height maintained at the midpoint of the conducting path. The towed array tubing around the conducting path was removed for some of the data points. A representative waveform with both the current and the acoustic pulse is shown in Figure 21. Nine data points were taken, and these are shown in Table 2.

27

TEST #	Voltage (V)	Pressure (Pa)	Distance (m)	Pressure at 1m (Pa)	Pulse Length (us)	Current Amplitude (A)	Current pulse length (us)
Test 3	0.246	18.92	0.27	5.11	160	191	110
Test 4	0.226	17.38	0.27	4.69	180	191	120
Test 5	0.223	17.15	0.27	4.63	180	189	120
Test 6	0.218	16.77	0.27	4.53	180	190	120
Test 7	0.19	14.62	0.27	3.95	130	194	110
Test 8	0.205	15.77	0.27	4.26	140	198	100
Test 9	0.289	22.23	0.27	6.00	140	not recorded	not recorded
Test 10	0.204	15.69	0.27	4.24	130	197	100

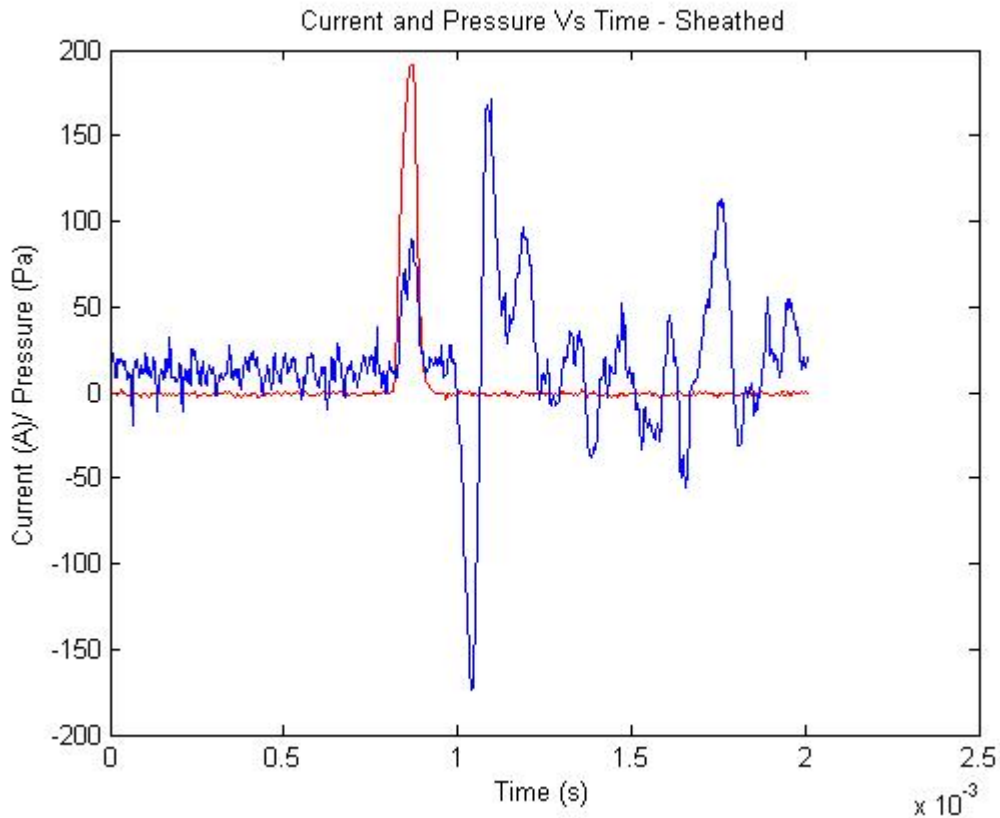Table 2.   Jan 25 Test Results

Figure 21.   Jan 25 NPS tank test zapper pulse with current waveform

B.   KEYPORT TEST

The testing of the zapper in seawater was done at Keyport, WA on January 20, 2006 at the Naval Undersea Warfare Center (NUWC) Acoustic Test Facility.   The purpose of this test was to test the zapper underwater and to see if the acoustic pulse was as expected and consistent with the NPS tests.   The zapper was deployed vertically underwater with a mechanical hoist and lowered several meters below the surface of the

water. An ITC 5600 type hydrophone was lowered to depth of the midpoint of the conducting path which was 4m. The hydrophone was initially placed 2m away. The conducting path was rotated in 90 degree increments to determine the waveform's directionality. The setup of the experiment is shown on Figure 22. The conducting path was raised and lowered 10cm above and below the level of the hydrophone and again, four samples were taken at 90 degree increments for each height. For these measurements, the hydrophone was moved to a distance of 1m from the conducting path. The zapper was then taken out of the water, the towed array tubing around the conducting path removed, and three measurements were taken at a distance of 2m. The hydrophone was again positioned at the midpoint of the conducting path. The sensitivity of the hydrophone was –166dB V/μPa. The temperature of the seawater was recorded as 9 degrees Celsius with a salinity of 29ppt. A waveform from this test is shown in Figure 23. A total of 15 pulses were recorded and the data is shown on Table 3.
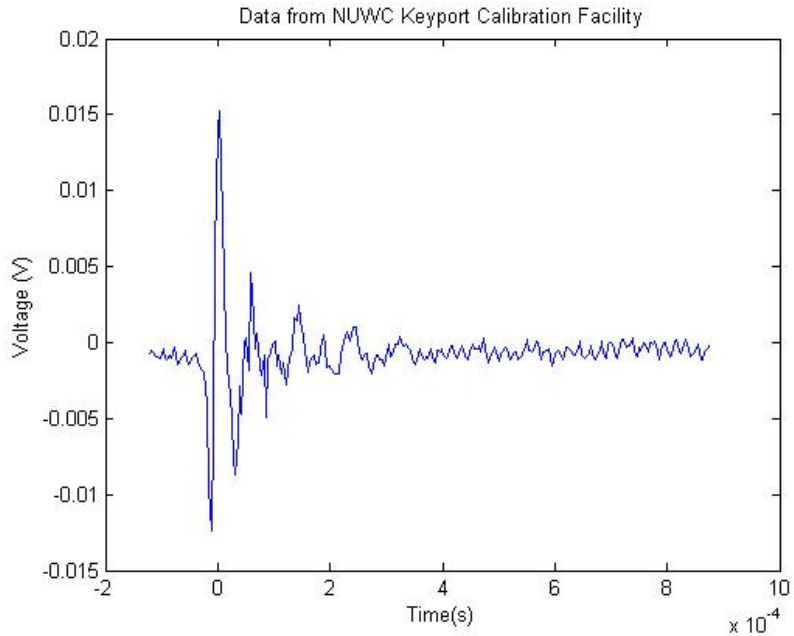

Figure 22.   NUWC Keyport Test

Figure 23.   NUWC Keyport zapper pulse

TEST #	Voltage (V)	Pressure (Pa)	Distance (m)	Pressure at 1m (Pa)	Pulse Length (us)
Test 1	1.27E-02	2.71E+00	2	5.42E+00	50
Test 2	1.72E-02	3.68E+00	2	7.35E+00	45
Test 3	1.38E-02	2.95E+00	2	5.90E+00	54
Test 4	1.66E-02	3.55E+00	2	7.09E+00	43
Test 5	9.93E-03	2.12E+00	1	2.12E+00	40
Test 6	8.74E-03	1.87E+00	1	1.87E+00	51
Test 7	9.00E-03	1.92E+00	1	1.92E+00	52
Test 8	8.54E-03	1.82E+00	1	1.82E+00	55
Test 9	4.70E-03	1.00E+00	1	1.00E+00	45
Test 10	3.81E-03	8.14E-01	1	8.14E-01	50
Test 11	6.06E-03	1.29E+00	1	1.29E+00	52
Test 12	6.09E-03	1.30E+00	1	1.30E+00	40
Test 13	8.09E-03	1.73E+00	2	3.46E+00	58
Test 14	7.60E-03	1.62E+00	2	3.25E+00	42
Test 15	7.25E-03	1.55E+00	2	3.10E+00	60

Table 3.   Keyport Test Results

30

VI. RESULTS

A. NPS TANK RESULTS

1. Jan 17 Test Results

As noted in Chapter V, the zapper produced an acoustic pulse that closely resembled the bipolar pulse that was expected but went negative first. In this initial test, the cause of this was not attributed to the pre-amplifier, as the inverter button was inactive. A series of tests were conducted to determine the polarity of the hydrophone. These tests revealed that the hydrophone was poled to produce a negative voltage for a positive pressure. As shown in Table 1, the peak pressure backed out to one meter varied widely and averaged 1.9 +/- 0.3 Pa. These pressures are about 100 times lower than the theoretical value of 308 Pa calculated using Eq 3. The gain of the pre-amplifier was set at 500. The reason for this large discrepancy is not yet known and is still being investigated. The pulse lengths were very close to the expected values as shown in Table 1. The average pulse lengths were 110 +/- 10μs, which is consistent with the theoretical value of 112μs.

2. Jan 25 Test Results

The second test at the NPS tank was done with a Pearson current monitor. When the current waveform and the acoustic pulse waveform are shown on the same graph as in Figure 22, an EMI spike is seen in the acoustic waveform at the same time as the current signal. As shown in Table 2, the average peak pressure was 4.7 +/- 0.6Pa. This value is also about two orders of magnitude below the theoretical value of 308 Pa. It is also inconsistent with the previous NPS tank pressure amplitude of 0.8Pa. Although the gain of the preamp was also recorded as 500 for this test, an error in the gain setting cannot be ruled out as a cause of this inconsistency. Other possibilities for this inconsistency include temperature and salinity variations between the two tests conducted at NPS. Unfortunately the temperature for these two tests was not recorded. Furthermore, not all of the salt added had a chance to dissolve in time for the tests on the 17th. Therefore the salinity was higher on the 25th. The average pulse lengths were considerably higher at 160 +/- 20μs, which is higher than the theoretical value of 112μs. The pressure

amplitude and pulse length did not change perceptibly when the conducting path insulation was removed.

The peak current measured with the conducting path insulation on averaged 191A. Using Ohm's law, V=IR, the resistance of the conducting path was calculated to be 12.5Ω. Applying Eq 4 the resistivity was calculated to be $0.17\Omega-m$, using the diameter of the copper conducting plates of 6cm. This resistivity of the tank was close to the accepted average resistivity of seawater, $0.2\Omega-m$. When the conducting path insulation was removed, the current increased to 198A. This corresponds to a resistance of 14Ω. Using Eq 4 and the resistivity of the tank, $0.17\Omega-m$, the effective diameter of the conducting path increased to 8cm. This effect is undoubtedly due to the fringing of the electric field and indicates that having insulation around the conducting path is valuable for concentrating the heat energy.

B.   KEYPORT TEST RESULTS

The four pulses that were that were recorded with the hydrophone in line with the midpoint of the conducting path are shown in Table 3. The average pressure of these are 6.4 +/- 0.9Pa. The pulse length did not appear to change with angle and averaged 49 +/- 6µs. These pulse amplitudes are the same order of magnitude as the NPS tests, but the average pulse length was about half the value measured at NPS. At this time it is not known whether the discrepancy is due to experimental procedure or experimental conditions. It is possible that during the NPS tests, the hydrophone was not positioned exactly on the acoustic axis of the zapper.

When the conducting path was raised and lowered 10cm, the average peak pressure lowered considerably to 1.5Pa. The angle between the hydrophone and the acoustic axis of the hydrophone was approximately 6 degrees. Based on Eq 3, the peak pulse amplitude at 6 degrees is expected to be about 2% of the on-axis amplitude. However, the measured peak pressures were approximately 20% of the on-axis values. This discrepancy cannot be attributed to near-field effects since the far-field should start at about 20cm based on the far-field equation:

Eq 7 $r = \dfrac{L^2}{4\lambda}$,

where L is the length of the conducting path and λ is the wavelength of the pulse.

Three pulses were recorded with the towed array tubing removed. The average of the peak pressure amplitudes was 3.3Pa which was approximately 3Pa lower than the average value when the conducting path insulation was on. Thus, the insulation appears to maximize the pressure amplitudes. A graph showing the peak pressure all of the waveforms recorded during both the NPS and Keyport tests as a function of range is shown in Figure 24. The curve on Figure 24 is the 1/r prediction based on the mean of the Keyport data.
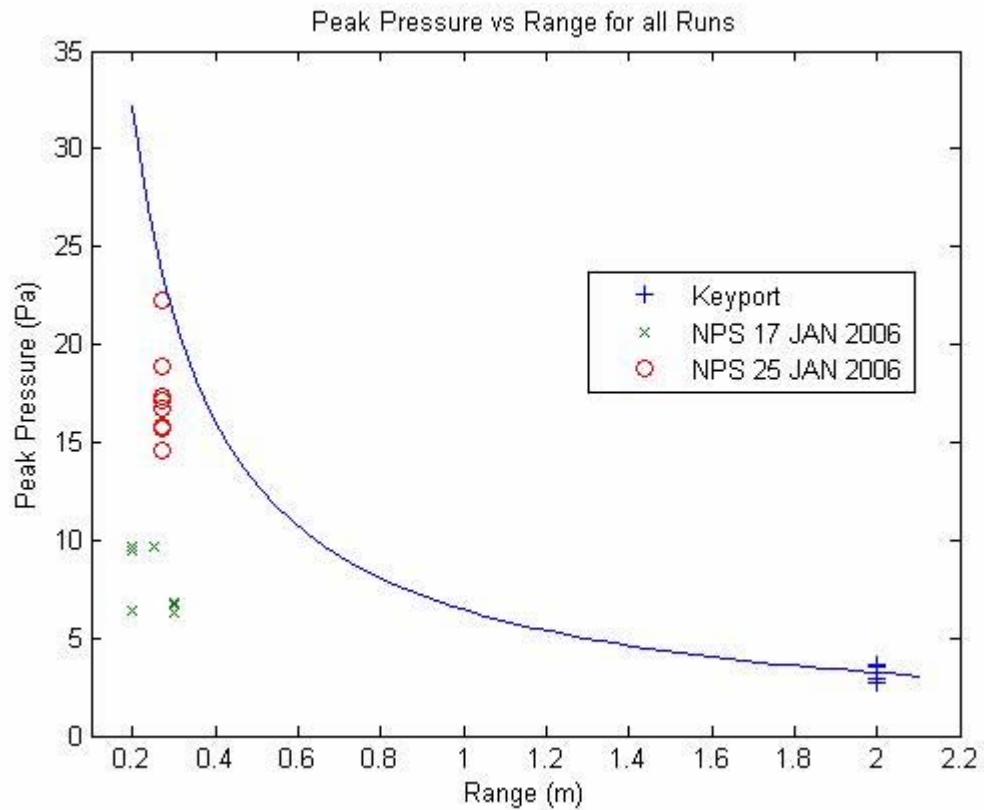
Figure 24.   Summary of Results - Peak Pressure vs. Range

THIS PAGE INTENTIONALLY LEFT BLANK

VII. CONCLUSION

A. DISCUSSION OF RESULTS

The zapper successfully produced a bipolar acoustic pulse. Qualitatively, this result validates the theory which predicts that a bipolar acoustic pulse is generated by the near instantaneous heating of a fluid. The pulse lengths measured in the NPS tank were reasonably consistent with the quantitative predictions of theory. They had an average value of 110μs and 160μs which is reasonably close to the theoretical value of 112μs. The pulse lengths recorded at Keyport were not consistent with theory. The average value of the pulse lengths was 49μs. The difference between the Keyport values and the theoretical value is being investigated. The simplest explanation for this discrepancy is a mistake in the recording of the sampling frequency. The pressure amplitudes for all the tests were fairly consistent and much lower than the predicted value of 308Pa.

The pressure amplitudes did not change significantly when the towed array tubing was removed from the conducting path in the NPS tank tests. However, when the same tests were done at Keyport, the differences in pressure were approximately 3Pa. This indicates that the towed array tubing does enhance the performance of the zapper, though perhaps not as dramatically as expected.

B. AREAS FOR FURTHER STUDY

While the zapper was successful in proving that the acoustic pulse created by an electric discharge in seawater is consistent with theoretical predictions for a neutrino interaction, there are still a number of unresolved questions. One of the more puzzling questions is the large difference between the measured pressure amplitude and the theoretical value. Another subject for further study is the difference that was seen between the NPS data and the Keyport data. More testing needs to be done to confirm that there is an actual difference in pulse length and amplitude rather than an incorrect
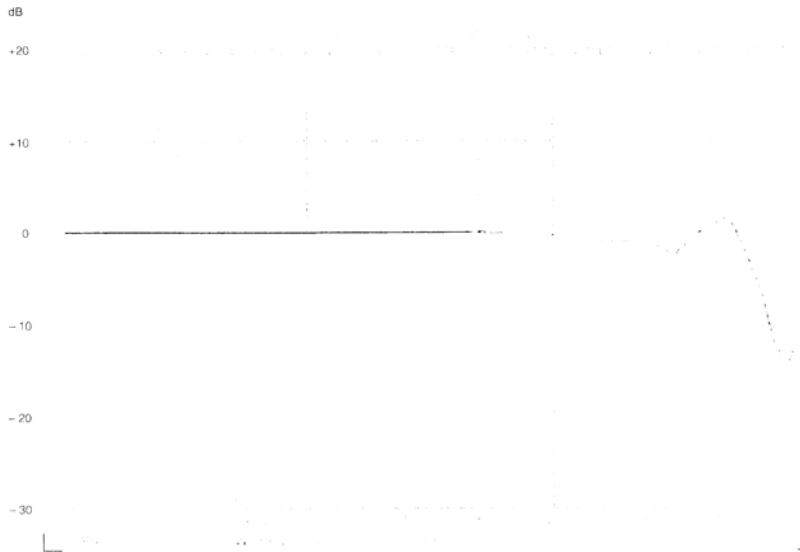
gain setting, calibration, or sampling rate. In addition, further work is necessary to determine the sensitivity of the pulse length and amplitude to temperature, depth, and salinity.

Follow on work also needs to be conducted to determine whether the amplitude of the zapper signal is strong enough to be used to calibrate the AHRP arrays.
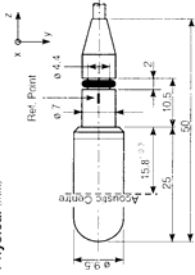
APPENDIX

Calibration Chart for Hydrophone Type 8103   Serial No.:2241680

MEASUREMENT SPECIALTIES

Model Description Code

Pressure Range

025	25 psig	003	= 3 bar
050	50 psig	005	= 5 bar
075	75 psig	007	= 7 bar
100	100 psig	010	= 10 bar
250	250 psig	035	= 35 bar
500	500 psig	070	= 70 bar
01K	1000 psig	175	= 175 bar
2K5	2500 psig	350	= 350 bar
05K	5000 psig	525	= 525 bar
7K5	7500 psig	700	= 700 bar
10K	10000 psig		

Pressure Units

P = psi
B = bar

Electrical Output

3   0.5 to 4.5 Vdc
4   1.0 to 5.0 Vdc
5   4-20 mVdc

Pressure Port

N	= 1/4" NPT
A	= 1/8" NPT
B	= 1/4 BSP
D	= 7/16-20 UNF
G	= M14x1.5 mm
H	= G 1/4"
I	= 1/2 NPT

Electrical Connection

1	2 ft. Cable
2	4 ft. Cable
3	10 ft. Cable
4	Packard Connector

EXAMPLE: MSP-600-500-P-3-N-1

Pressure range
Pressure units
Electrical output
Pressure port
Electrical connection

WARNING: READ BEFORE INSTALLATION

When using this transducer, carefully read the instructions before installing and operating this product. Ensure that you use the correct electrical connections and pressure ranges as noted in this instruction sheet. Do not subject this transducer to pressure spikes in excess of the maximum pressure specification. Failure to do so could result in personal and damage to the transducer.

Supply	5 Vdc (4.75-5.25)	Output	0.5 - 4.5 Vdc (ratiometric)

Output Type - 3

Voltage Output Sensor Wiring Configuration
(Single-Ended/Amplified Output)

Supply	10-30 Vdc	Output	1-5 Vdc (Fixed)

Output Type - 4

Voltage Output Sensor Wiring Configuration
(Single-Ended/Amplified Output)

Supply	10-30 Vdc	Output	4-20 mAdc (Two-Wire)

Output Type - 5

Current Output
Sensor Wiring Configuration

Packard Connector Type -3 & -4
Pin A - Supply
Pin B - GND
Pin C - Output

Packard Connector Type -5
Pin A - Supply
Pin B - Output
Pin C - Not used

* Packard Mating Connector
1 ea. - Housing p/n: 12078090
3 ea. - Pins p/n: 12103881-L

Cable Output, Type -3 & -4
Red - Supply
Black - GND
White - Output
Green - Not used
Bare - Drain (connects to chassis)

Cable Output, Type -5
Red - Supply
Black - Output
White - Not used
Green - Not used
Bare - Drain (connects to chassis)
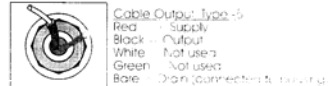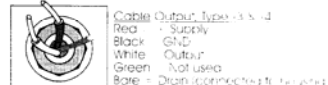
Performance Specifications

Accuracy (combined linearity, hysteresis and repeatability)	±0.25% BSL, max (per ISA S37.2)
Media compatibility	17-4 PH stainless steel, (316 stainless steel available upon request)
Pressure overload	2x rated pressure
Burst pressure	5x full scale or 20,000 psi, whichever is less
Long term stability (1 year)	±0.25% of FS Span (Typical)

Electrical

Load impedance	For voltage output configurations use > 100K Ohms for quoted performance. For 4-20 mA output configuration use 0.05*(Vsupply-10) K Ohms for max loop resistance.
Bandwidth (-3dB)	DC to 1 Khz (Typical)
Operating temp range	-40° to 212°F (-40° to 100°C) for cable configuration -40° to 257°F (-40° to 125°C) for Packard - style connector configuration
Compensated temp range	4° to 185°F (-20° to 85°C)
Total error band (over compensated temperature range)	< ±1% of FS (75-10,000 PSI), < ±1.5% of FS (25-50 PSI)
(over full operating temperature range)	< ±1.5% of FS (-40° to 125°C)
Storage temperature range	-49° to 212°F (-45° to 100°C) for cable configuration -49° to 257°F (-45° to 125°C) for Packard - style connector configuration
Shock	50g, 11 msec half sine shock per MIL-STD- 202F, method 213B, condition A
Vibration	±20g MIL-STD-810C, Procedure 514.2, Figure 514.2-2, curve L
EMI/RFI	EN 50081-2 EN 50082-2 (10 V/M, 26-1000 Mhz) EN 61326 (Effective July 1, 2001)

Note: All performance and electrical specifications are referenced to 25°C, unless otherwise indicated.

Dear valued Customer:

The enclosed pressure transducer has been manufactured, tested and inspected in accordance with all applicable procedures and practices as established in our registered ISO 9000 quality system. We certify that this sensor is in full conformance with all written specifications as contained in this instruction sheet.
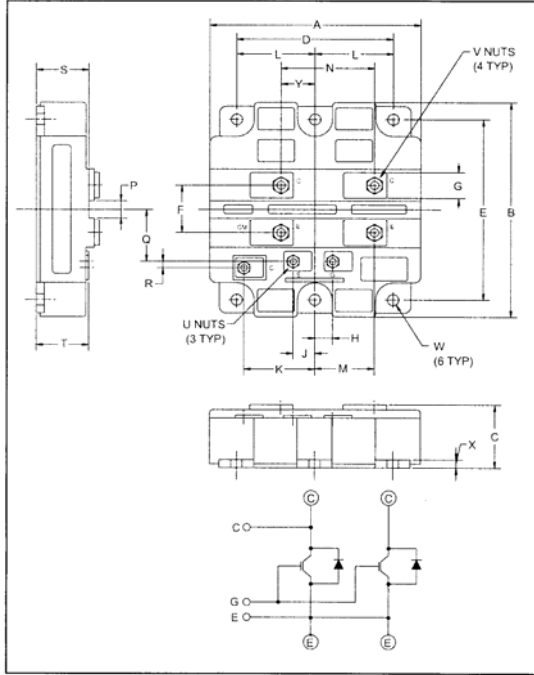
Signature: Wang Xuemin
Title: Quality Manager, MSI/JL

POWEREX

**Single IGBTMOD™
HVIGBT
400 Amperes/4500 Volts**

Outline Drawing and Circuit Diagram

Description:
Powerex IGBTMOD™ Modules are designed for use in switching applications. Each module consists of one IGBT Transistor with a reverse-connected super-fast recovery free-wheel diode.
All components and interconnects are isolated from the heat sinking baseplate, offering simplified system assembly and thermal management.

Features:
☐ Low Drive Power
☐ Low $V_{CE(sat)}$
☐ Super-Fast Recovery Free-Wheel Diode
☐ Isolated Baseplate for Easy Heat Sinking

Applications:
☐ Traction
☐ Medium Voltage Drive
☐ High Voltage Power Supplies

Ordering Information:
Example: Select the complete part module number you desire from the table below -i.e. CM400HB-90H is a 4500V (V_{CES}), 400 Ampere Single IGBTMOD™ Power Module.

Type	Current Rating Amperes	V_{CES} Volts (x 50)
CM	400	90

Dimensions	Inches	Millimeters
A	5.12	130.0
B	5.51	140.0
C	1.50	38.0
D	4.48	114.0
E	4.88±0.01	124.0±0.25
F	1.57	40.0
G	0.79	20.0
H	0.41	10.35
J	0.42	10.65
K	1.92	48.8
L	2.24±0.01	57.0±0.25
M	1.71	43.5

Dimensions	Inches	Millimeters
N	2.42	61.5
P	0.59	15.0
Q	1.57	40.0
R	0.20	5.2
S	1.16	29.5
T	1.10	28.0
U	M4 Metric	M4
V	M8 Metric	M8
W	0.28 Dia.	Dia.7.0
X	0.20	5.0
Y	0.71	18.0

1

CM400HB-90H
Single IGBTMOD™ HVIGBT
400 Amperes/4500 Volts

Absolute Maximum Ratings, T_j = 25 °C unless otherwise specified

Ratings	Symbol	CM400HB-90H	Units
Junction Temperature	T_j	-40 to 150	°C
Storage Temperature	T_{stg}	-40 to 125	°C
Collector-Emitter Voltage (V_{GE} = 0V)	V_{CES}	4500	Volts
Gate-Emitter Voltage (V_{CE} = 0V)	V_{GES}	±20	Volts
Collector Current (T_C = 25°C)	I_C	400	Amperes
Peak Collector Current (Pulse)	I_{CM}	800*	Amperes
Diode Forward Current** (T_C = 25°C)	I_E	400	Amperes
Diode Forward Surge Current** (Pulse)	I_{EM}	800*	Amperes
Maximum Collector Dissipation (T_C = 25°C, IGBT Part, $T_j \leq$ 125°C)	P_C	4300	Watts
Max. Mounting Torque M8 Terminal Screws	–	115	in-lb
Max. Mounting Torque M6 Mounting Screws	–	53	in-lb
Max. Mounting Torque M4 Auxiliary Terminal Screws	–	17	in-lb
Module Weight (Typical)	–	1.5	kg
Isolation Voltage (Charged Part to Baseplate, AC 60Hz 1 min.)	V_{iso}	6000	Volts

* Pulse width and repetition rate should be such that device junction temperature (T_j) does not exceed $T_{j(max)}$ rating.
**Represents characteristics of the anti-parallel, emitter-to-collector free-wheel diode (FWDi).

Static Electrical Characteristics, T_j = 25 °C unless otherwise specified

Characteristics	Symbol	Test Conditions	Min.	Typ.	Max.	Units
Collector-Cutoff Current	I_{CES}	V_{CE} = V_{CES}, V_{GE} = 0V	–	–	8.0	mA
Gate Leakage Current	I_{GES}	V_{GE} = V_{GES}, V_{CE} = 0V	–	–	0.5	μA
Gate-Emitter Threshold Voltage	$V_{GE(th)}$	I_C = 40mA, V_{CE} = 10V	4.5	6.0	7.5	Volts
Collector-Emitter Saturation Voltage	$V_{CE(sat)}$	I_C = 400A, V_{GE} = 15V, T_j = 25°C	–	3.0	3.9*	Volts
		I_C = 400A, V_{GE} = 15V, T_j = 125°C	–	3.3	–	Volts
Total Gate Charge	Q_G	V_{CC} = 2250V, I_C = 400A, V_{GE} = 15V	–	3.6	–	μC
Emitter-Collector Voltage**	V_{EC}	I_E = 400A, V_{GE} = 0V	–	4.0	5.2	Volts

* Pulse width and repetition rate should be such that device junction temperature rise is negligible.
**Represents characteristics of the anti-parallel, emitter-to-collector free-wheel diode (FWDi).

2

CM400HB-90H
Single IGBTMOD™ HVIGBT
400 Amperes/4500 Volts

Dynamic Electrical Characteristics, T_j = 25 °C unless otherwise specified

Characteristics		Symbol	Test Conditions	Min.	Typ.	Max.	Units
Input Capacitance		C_{ies}		–	72	–	nF
Output Capacitance		C_{oes}	V_{GE} = 0V, V_{CE} = 10V	–	5.3	–	nF
Reverse Transfer Capacitance		C_{res}		–	1.6	–	nF
Resistive	Turn-on Delay Time	$t_{d(on)}$	V_{CC} = 2250V, I_C = 400A,	–	–	2.4	µs
Load	Rise Time	t_r	V_{GE1} = V_{GE2} = 15V,	–	–	2.4	µs
Switching	Turn-off Delay Time	$t_{d(off)}$	R_G = 22.5Ω	–	–	6.0	µs
Times	Fall Time	t_f	Resistive Load Switching Operation	–	–	1.2	µs
Diode Reverse Recovery Time**		t_{rr}	I_E = 400A, di_E/dt = -800A/µs	–	–	1.8	µs
Diode Reverse Recovery Charge**		Q_{rr}	I_E = 400A, di_E/dt = -800A/µs	–	160*	–	µC

* Pulse width and repetition rate should be such that device junction temperature rise is negligible.
**Represents characteristics of the anti-parallel, emitter-to-collector free-wheel diode (FWDi).

Thermal and Mechanical Characteristics, T_j = 25 °C unless otherwise specified

Characteristics	Symbol	Test Conditions	Min.	Typ.	Max.	Units
Thermal Resistance, Junction to Case	$R_{th(j-c)}$ Q	Per IGBT	–	–	0.023	K/W
Thermal Resistance, Junction to Case	$R_{th(j-c)}$ D	Per FWDi	–	–	0.045	K/W
Contact Thermal Resistance, Case to Fin	$R_{th(c-f)}$	Per Module, Thermal Grease Applied	–	0.015	–	K/W

3

CM400HB-90H
Single IGBTMOD™ HVIGBT
400 Amperes/4500 Volts

4

43
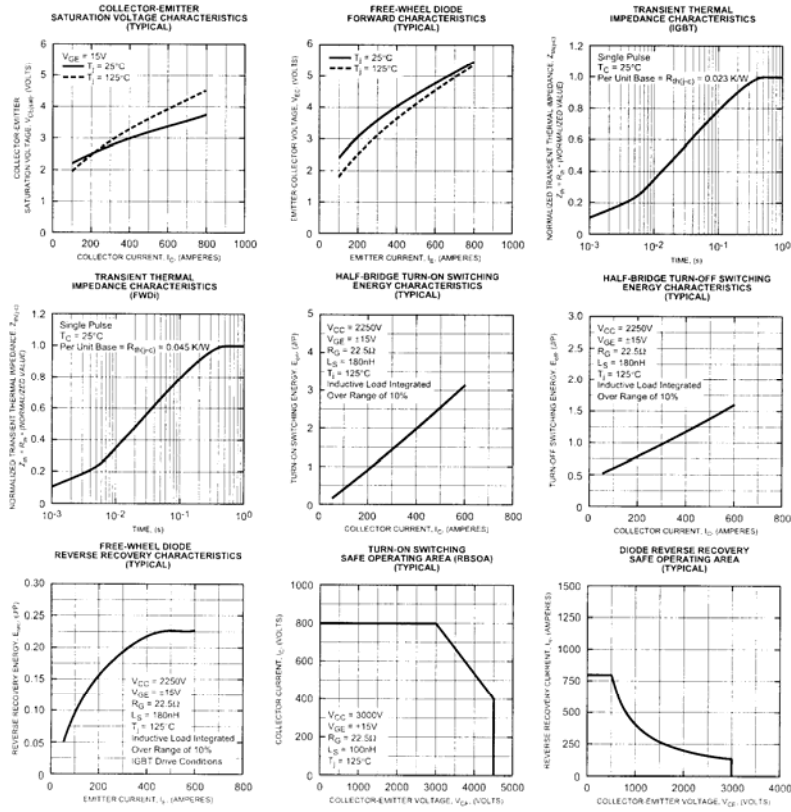
Compact, Low Cost High Voltage Converter

1.5kV to 25kV (Positive or Negative) @ 1.5 Watts
DX Series

www.emcohighvoltage.com

EMCO
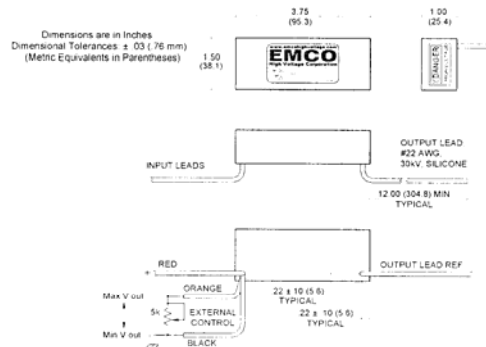High Voltage Corporation

The DX series is a line of compact power supplies providing up to 25,000 VDC for air cleaners, igniters, dielectric testers, electrostatic field generators and other applications requiring a compact source of clean, reliable, low cost high voltage. This unit exhibits low noise and EMI/RFI by utilizing a quasi-sinewave oscillator and a fully enclosed ferrite pot core transformer. The output voltage is controlled by an external potentiometer or resistor. Both positive and negative outputs are available. The high voltage connection is made through a 30kV silicone wire. Call, fax, or e-mail your requirements for immediate attention.

FEATURES
Resistance Controllable
Low EMI/RFI Sinewave Oscillator
Small Size
Short Circuit Protection
Low Cost/High Performance

OPTIONS
24V Input
Input/Output Connectors
Input/Output Isolation
Voltage Monitor

APPLICATIONS
Air cleaners
Igniters
Dielectric Testers
Ionizers
Electrostatic Generators
CRT Anodes
Image Intensifiers
Capacitor Charging

PHYSICAL CHARACTERISTICS
SIZE: 3.75 x 1.5 x 1 (95.3 x 38.1 x 25.4)
WEIGHT: 7 Ounces (198 grams)
PACKAGING: Fully Encapsulated
CASE MATERIAL: Glass-filled Epoxy
HV OUTPUT LEAD: #22 AWG, 30kV, Silicone

ELECTRICAL SPECIFICATIONS
INPUT VOLTAGE: 12 Volts (-5%, +10%)
INPUT CURRENT, FULL LOAD: <400 mA
OUTPUT VOLTAGE: *See Table*
OUTPUT CURRENT: *See Table*
RIPPLE: 2% P-P
VOLTAGE CONTROL: Connect 5k Potentiometer with wiper arm to orange wire. Connect remaining potentiometer lead to black wire.
OPERATING TEMP: -10° to +50° C

MODEL	OUTPUT VOLTAGE	OUTPUT[*1] CURRENT
DX100	1.5kV to 10kV	100 uA
DX100N	-1.5kV to -10kV	100 uA
DX120	1.8kV to 12kV	100 uA
DX120N	-1.8kV to -12kV	100 uA
DX150	2.5kV to 15kV	100 uA
DX150N	-2.5kV to -15kV	100 uA
DX200	3kV to 20kV	75 uA
DX200N	-3kV to -20kV	75 uA
DX250	4kV to 25kV	75 uA
DX250N	-4kV to -25kV	75 uA
DX250N-24[*2]	-10kV to -25kV	75 uA

WIRE COLOR	AWG	FUNCTION
Red	22	(+) Input
Black	22	Ground (Input Output)
Orange	22	Voltage Control
30kV Silicone	22	HV Output

TIP: LEAVE ORANGE WIRE DISCONNECTED AND VARY THE INPUT VOLTAGE FOR PROPORTIONAL OPERATION.

*Note
1. At Maximum Rated Output Voltage.
2. 24V Input Power Option

Dimensions are in Inches
Dimensional Tolerances ± .03 (.76 mm)
(Metric Equivalents in Parentheses)

We reserve the right to make changes without notification

4717P

International **IⱤR** Rectifier

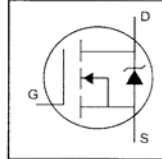**AUTOMOTIVE MOSFET**

IRF2805

HEXFET® Power MOSFET

Typical Applications
- Climate Control, ABS, Electronic Braking, Windshield Wipers

Features
- Advanced Process Technology
- Ultra Low On-Resistance
- 175°C Operating Temperature
- Fast Switching
- Repetitive Avalanche Allowed up to Tjmax

$V_{DSS} = 55V$

$R_{DS(on)} = 4.7m\Omega$

$I_D = 75A$

Description
Specifically designed for Automotive applications, this HEXFET® Power MOSFET utilizes the latest processing techniques to achieve extremely low on-resistance per silicon area. Additional features of this design are a 175°C junction operating temperature, fast switching speed and improved repetitive avalanche rating. These features combine to make this design an extremely efficient and reliable device for use in Automotive applications and a wide variety of other applications.

TO-220AB
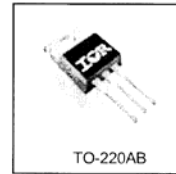
Absolute Maximum Ratings

	Parameter	Max.	Units
I_D @ T_C = 25°C	Continuous Drain Current, V_{GS} @ 10V (Silicon limited)	175	
I_D @ T_C = 100°C	Continuous Drain Current, V_{GS} @ 10V (See Fig.9)	120	A
I_D @ T_C = 25°C	Continuous Drain Current, V_{GS} @ 10V (Package limited)	75	
I_{DM}	Pulsed Drain Current ①	700	
P_D @T_C = 25°C	Power Dissipation	330	W
	Linear Derating Factor	2.2	W/°C
V_{GS}	Gate-to-Source Voltage	± 20	V
E_{AS}	Single Pulse Avalanche Energy②	450	mJ
E_{AS} (6 sigma)	Single Pulse Avalanche Energy Tested Value②	1220	
I_{AR}	Avalanche Current①	See Fig.12a, 12b, 15, 16	A
E_{AR}	Repetitive Avalanche Energy①		mJ
T_J	Operating Junction and	-55 to + 175	
T_{STG}	Storage Temperature Range		°C
	Soldering Temperature, for 10 seconds	300 (1.6mm from case)	
	Mounting Torque, 6-32 or M3 screw	1.1 (10)	N•m (lbf•in)

Thermal Resistance

	Parameter	Typ.	Max.	Units
$R_{\theta JC}$	Junction-to-Case	——	0.45	
$R_{\theta CS}$	Case-to-Sink, Flat, Greased Surface	0.50	——	°C/W
$R_{\theta JA}$	Junction-to-Ambient	——	62	

HEXFET(R) is a registered trademark of International Rectifier.

www.irf.com

1

8/8/02

45

IRF2805

Electrical Characteristics @ T_J = 25°C (unless otherwise specified)

	Parameter	Min.	Typ.	Max.	Units	Conditions
$V_{(BR)DSS}$	Drain-to-Source Breakdown Voltage	55	——	——	V	V_{GS} = 0V, I_D = 250µA
$\Delta V_{(BR)DSS}/\Delta T_J$	Breakdown Voltage Temp. Coefficient	——	0.06	——	V/°C	Reference to 25°C, I_D = 1mA
$R_{DS(on)}$	Static Drain-to-Source On-Resistance	——	3.9	4.7	mΩ	V_{GS} = 10V, I_D = 104A ④
$V_{GS(th)}$	Gate Threshold Voltage	2.0	——	4.0	V	V_{DS} = 10V, I_D = 250µA
g_{fs}	Forward Transconductance	91	——	——	S	V_{DS} = 25V, I_D = 104A
I_{DSS}	Drain-to-Source Leakage Current	——	——	20	µA	V_{DS} = 55V, V_{GS} = 0V
		——	——	250		V_{DS} = 55V, V_{GS} = 0V, T_J = 125°C
I_{GSS}	Gate-to-Source Forward Leakage	——	——	200	nA	V_{GS} = 20V
	Gate-to-Source Reverse Leakage	——	——	-200		V_{GS} = -20V
Q_g	Total Gate Charge	——	150	230		I_D = 104A
Q_{gs}	Gate-to-Source Charge	——	38	57	nC	V_{DS} = 44V
Q_{gd}	Gate-to-Drain ("Miller") Charge	——	52	78		V_{GS} = 10V④
$t_{d(on)}$	Turn-On Delay Time	——	14	——		V_{DD} = 28V
t_r	Rise Time	——	120	——	ns	I_D = 104A
$t_{d(off)}$	Turn-Off Delay Time	——	68	——		R_G = 2.5Ω
t_f	Fall Time	——	110	——		V_{GS} = 10V ④
L_D	Internal Drain Inductance	——	4.5	——	nH	Between lead, 6mm (0.25in.) from package and center of die contact
L_S	Internal Source Inductance	——	7.5	——		
C_{iss}	Input Capacitance	——	5110	——		V_{GS} = 0V
C_{oss}	Output Capacitance	——	1190	——	pF	V_{DS} = 25V
C_{rss}	Reverse Transfer Capacitance	——	210	——		f = 1.0MHz, See Fig. 5
C_{oss}	Output Capacitance	——	6470	——		V_{GS} = 0V, V_{DS} = 1.0V, f = 1.0MHz
C_{oss}	Output Capacitance	——	860	——		V_{GS} = 0V, V_{DS} = 44V, f = 1.0MHz
C_{oss} eff.	Effective Output Capacitance ②	——	1600	——		V_{GS} = 0V, V_{DS} = 0V to 44V

Source-Drain Ratings and Characteristics

	Parameter	Min.	Typ.	Max.	Units	Conditions
I_S	Continuous Source Current (Body Diode)	——	——	175	A	MOSFET symbol showing the integral reverse p-n junction diode.
I_{SM}	Pulsed Source Current (Body Diode) ①	——	——	700		
V_{SD}	Diode Forward Voltage	——	——	1.3	V	T_J = 25°C, I_S = 104A, V_{GS} = 0V ④
t_{rr}	Reverse Recovery Time	——	80	120	ns	T_J = 25°C, I_F = 104A
Q_{rr}	Reverse Recovery Charge	——	290	430	nC	di/dt = 100A/µs ④
t_{on}	Forward Turn-On Time	Intrinsic turn-on time is negligible (turn-on is dominated by L_S+L_D)				

Notes:

① Repetitive rating; pulse width limited by max. junction temperature. (See fig. 11).

② Starting T_J = 25°C, L = 0.08mH R_G = 25Ω, I_{AS} = 104A. (See Figure 12).

③ I_{SD} ≤ 104A, di/dt ≤ 240A/µs, V_{DD} ≤ $V_{(BR)DSS}$, T_J ≤ 175°C

④ Pulse width < 400µs; duty cycle ≤ 2%.

⑤ C_{oss} eff. is a fixed capacitance that gives the same charging time as C_{oss} while V_{DS} is rising from 0 to 80% V_{DSS}.

⑥ Limited by T_{Jmax}, see Fig.12a, 12b, 15, 16 for typical repetitive avalanche performance.

⑦ This value determined from sample failure population. 100% tested to this value in production.
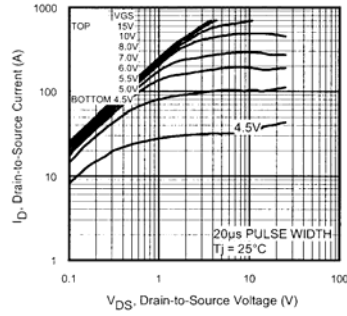
www.irf.com
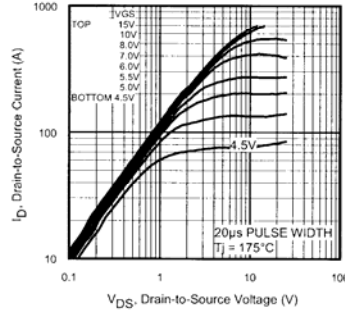
Fig 1. Typical Output Characteristics
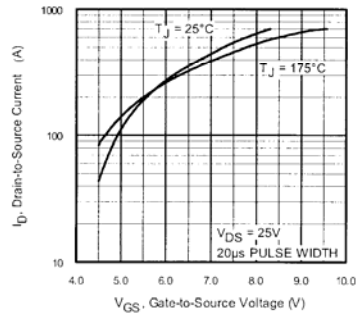

Fig 2. Typical Output Characteristics

Fig 3. Typical Transfer Characteristics

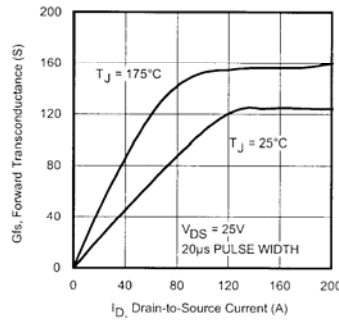Fig 4. Typical Forward Transconductance
Vs. Drain Current
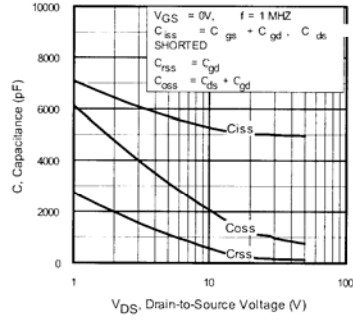
www.irf.com

3

47

IRF2805

Fig 5. Typical Capacitance Vs.
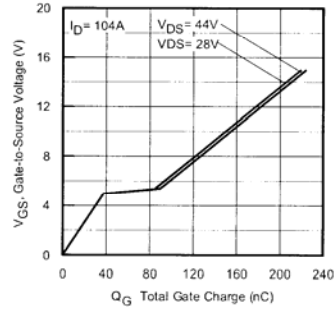Drain-to-Source Voltage
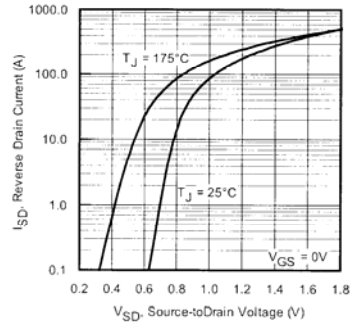

Fig 6. Typical Gate Charge Vs.
Gate-to-Source Voltage

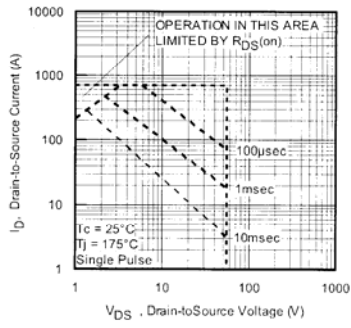

Fig 7. Typical Source-Drain Diode
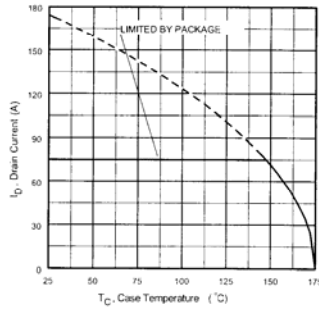Forward Voltage

Fig 8. Maximum Safe Operating Area
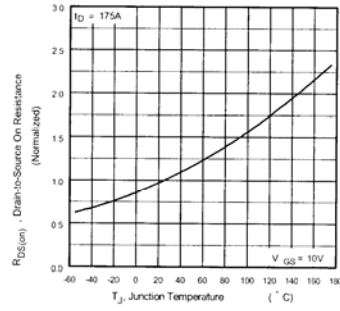
4

48

Fig 9. Maximum Drain Current Vs.
Case Temperature

Fig 10. Normalized On-Resistance
Vs. Temperature
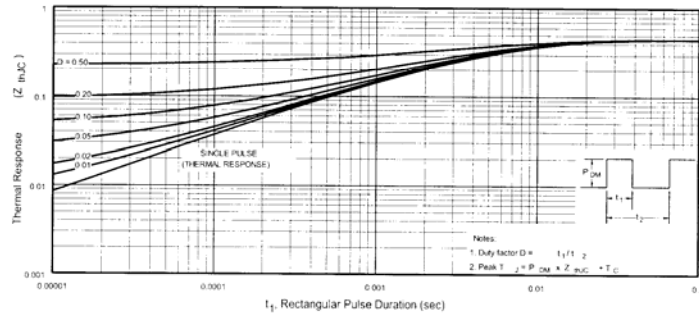

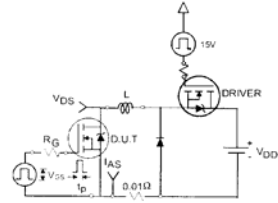Fig 11. Maximum Effective Transient Thermal Impedance, Junction-to-Case

49

IRF2805

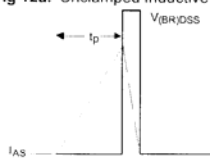**Fig 12a.** Unclamped Inductive Test Circuit

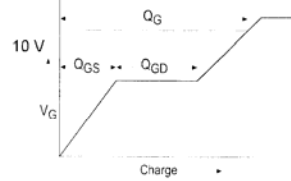**Fig 12b.** Unclamped Inductive Waveforms

Fig 13a. Basic Gate Charge Waveform
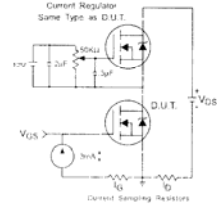

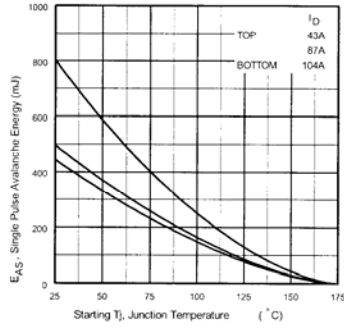**Fig 13b.** Gate Charge Test Circuit

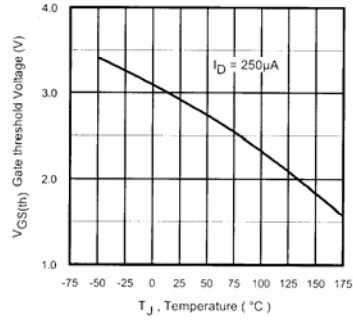**Fig 12c.** Maximum Avalanche Energy
Vs. Drain Current

Fig 14. Threshold Voltage Vs. Temperature
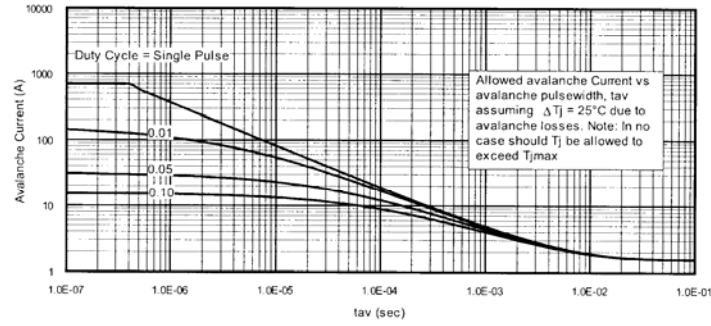
www.irf.com

6

50

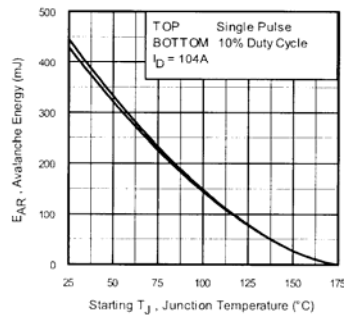Fig 15. Typical Avalanche Current Vs.Pulsewidth

Fig 16. Maximum Avalanche Energy
Vs. Temperature

www.irf.com

Notes on Repetitive Avalanche Curves , Figures 15, 16:
(For further info, see AN-1005 at www.irf.com)
1. Avalanche failures assumption:
   Purely a thermal phenomenon and failure occurs at a
   temperature far in excess of T_{jmax}. This is validated for
   every part type.
2. Safe operation in Avalanche is allowed as long as T_{jmax} is
   not exceeded.
3. Equation below based on circuit and waveforms shown in
   Figures 12a, 12b.
4. $P_{D\ (ave)}$ = Average power dissipation per single
   avalanche pulse.
5. BV = Rated breakdown voltage (1.3 factor accounts for
   voltage increase during avalanche).
6. I_{av} = Allowable avalanche current.
7. ΔT = Allowable rise in junction temperature, not to exceed
   T_{jmax} (assumed as 25°C in Figure 15, 16).
   t_{av} = Average time in avalanche.
   D = Duty cycle in avalanche = $t_{av} \cdot f$
   $Z_{thJC}(D, t_{av})$ = Transient thermal resistance, see figure 11)

$$P_{D\ (ave)} = 1/2\ (\ 1.3 \cdot BV \cdot I_{av}) = \Delta T / Z_{thJC}$$
$$I_{av} = 2\ \Delta T / [1.3 \cdot BV \cdot Z_{th}]$$
$$E_{AS\ (AR)} = P_{D\ (ave)} \cdot t_{av}$$
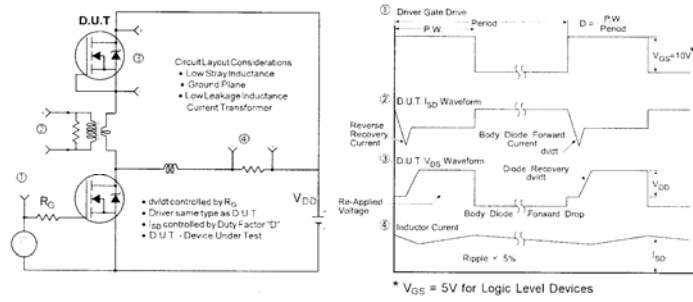
7

51

International
IOR Rectifier

Fig 17. Peak Diode Recovery dv/dt Test Circuit for N-Channel
HEXFET® Power MOSFETs
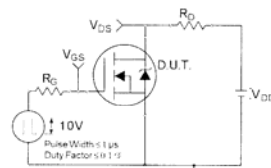
Fig 18a. Switching Time Test Circuit
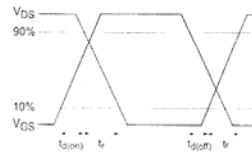
Fig 18b. Switching Time Waveforms

www.irf.com

52

TO-220AB Package Outline
Dimensions are shown in millimeters (inches)

LEAD ASSIGNMENTS
1 - GATE
2 - DRAIN
3 - SOURCE
4 - DRAIN
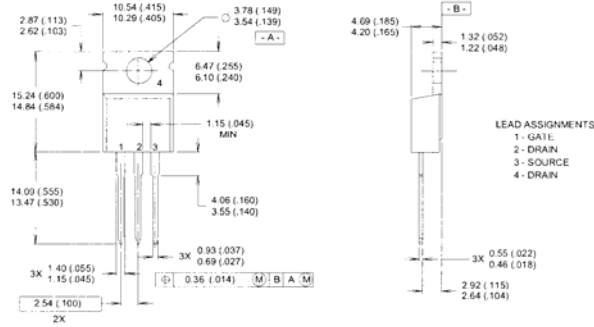
NOTES:
1 DIMENSIONING & TOLERANCING PER ANSI Y14.5M, 1982.
2 CONTROLLING DIMENSION : INCH

3 OUTLINE CONFORMS TO JEDEC OUTLINE TO-220AB
4 HEATSINK & LEAD MEASUREMENTS DO NOT INCLUDE BURRS

TO-220AB Part Marking Information

EXAMPLE: THIS IS AN IRF1010
LOT CODE 1789
ASSEMBLED ON WW 19, 1997
IN THE ASSEMBLY LINE "C"

INTERNATIONAL RECTIFIER LOGO

PART NUMBER

ASSEMBLY LOT CODE

DATE CODE
YEAR 7 – 1997
WEEK 19
LINE C
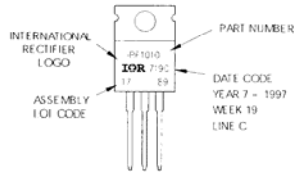
Data and specifications subject to change without notice.
This product has been designed and qualified for the Automotive [Q101] market.
Qualification Standards can be found on IR's Web site.

International
IΩR Rectifier

POSITIVE VOLTAGE REGULATORS

- OUTPUT CURRENT UP TO 1.5 A
- OUTPUT VOLTAGES OF 5; 5.2; 6; 8; 8.5; 9; 12; 15; 18; 24V
- THERMAL OVERLOAD PROTECTION
- SHORT CIRCUIT PROTECTION
- OUTPUT TRANSITION SOA PROTECTION

DESCRIPTION

The L7800 series of three-terminal positive regulators is available in TO-220 ISOWATT220 TO-3 and D²PAK packages and several fixed output voltages, making it useful in a wide range of applications. These regulators can provide local on-card regulation, eliminating the distribution problems associated with single point regulation. Each type employs internal current limiting, thermal shut-down and safe area protection, making it essentially indestructible. If adequate heat sinking is provided, they can deliver over 1A output current. Although designed primarily as fixed voltage regulators, these devices can be used with external components to obtain adjustable voltages and currents.

TO-3   D²PAK

TO-220   ISOWATT220

BLOCK DIAGRAM

54
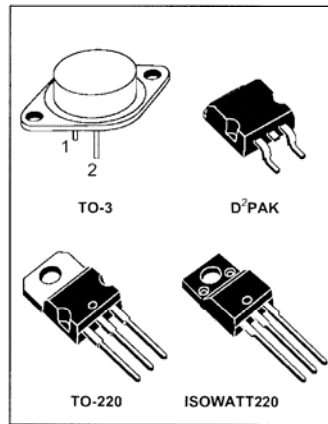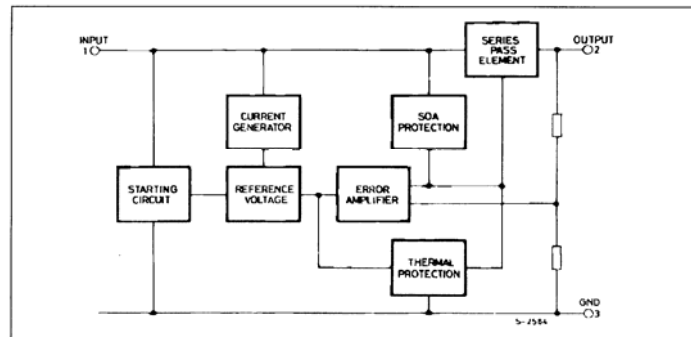
ABSOLUTE MAXIMUM RATINGS

Symbol	Parameter	Value	Unit
V_i	DC Input Voltage (for V_O = 5 to 18V)	35	V
	(for V_O = 20, 24V)	40	V
I_o	Output Current	Internally limited	
P_{tot}	Power Dissipation	Internally limited	
T_{op}	Operating Junction Temperature Range (for L7800)	-55 to 150	°C
	(for L7800C)	0 to 150	°C
T_{stg}	Storage Temperature Range	-65 to 150	°C

THERMAL DATA

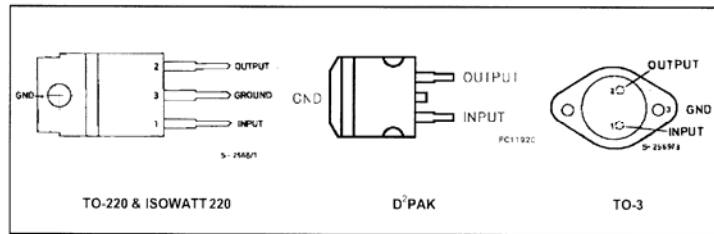| Symbol	Parameter		D^2PAK	TO-220	ISOWATT220	TO-3	Unit
$R_{thj-case}$	Thermal Resistance Junction-case	Max	3	3	4	4	°C/W
$R_{thj-amb}$	Thermal Resistance Junction-ambient	Max	62.5	50	60	35	°C/W

CONNECTION DIAGRAM AND ORDERING NUMBERS (top view)

TO-220 & ISOWATT 220 D^2PAK   TO-3

Type	TO-220	D^2PAK (*)	ISOWATT220	TO-3	Output Voltage
L7805				L7805T	5V
L7805C	L7805CV	L7805CD2T	L7805CP	L7805CT	5V
L7852C	L7852CV	L7852CD2T	L7852CP	L7852CT	5.2V
L7806				L7806T	6V
L7806C	L7806CV	L7806CD2T	L7806CP	L7806CT	6V
L7808				L7808T	8V
L7808C	L7808CV	L7808CD2T	L7808CP	L7808CT	8V
L7885C	L7885CV	L7885CD2T	L7885CP	L7885CT	8.5V
L7809C	L7809CV	L7809CD2T	L7809CP	L7809CT	9V
L7812				L7812T	12V
L7812C	L7812CV	L7812CD2T	L7812CP	L7812CT	12V
L7815				L7815T	15V
L7815C	L7815CV	L7815CD2T	L7815CP	L7815CT	15V
L7818				L7818T	18V
L7818C	L7818CV	L7818CD2T	L7818CP	L7818CT	18V
L7820				L7820T	20V
L7820C	L7820CV	L7820CD2T	L7820CP	L7820CT	20V
L7824				L7824T	24V
L7824C	L7824CV	L7824CD2T	L7824CP	L7824CT	24V

(*) AVAILABLE IN TAPE AND REEL WITH "-TR" SUFFIX

55

APPLICATION CIRCUIT
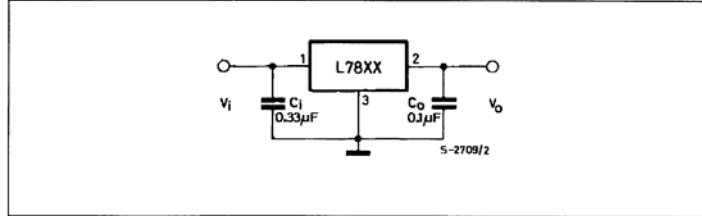
SCHEMATIC DIAGRAM

56
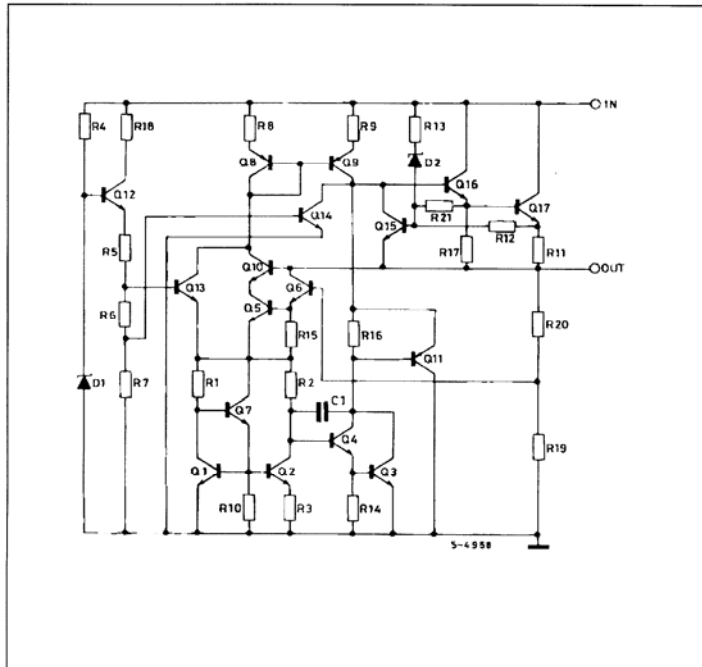
TEST CIRCUITS

Figure 1 : DC Parameter

Figure 2 : Load Regulation.

Figure 3 : Ripple Rejection.

57

ELECTRICAL CHARACTERISTICS FOR L7805C (refer to the test circuits, T_j = 0 to 125 °C, V_i = 10V, I_o = 500 mA, C_i = 0.33 µF, C_o = 0.1 µF unless otherwise specified)

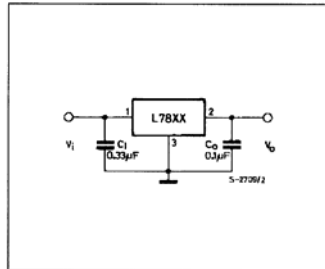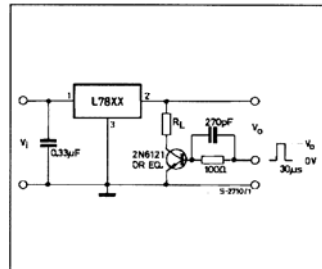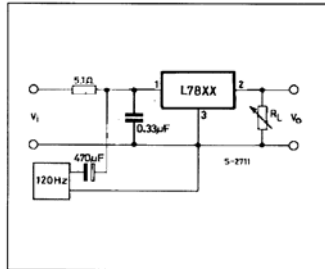| Symbol	Parameter	Test Conditions	Min.	Typ.	Max.	Unit
V_o	Output Voltage	T_j = 25 °C	4.8	5	5.2	V
V_o	Output Voltage	I_o = 5 mA to 1 A $P_o \leq$ 15 W V_i = 7 to 20 V	4.75	5	5.25	V
ΔV_o*	Line Regulation	V_i = 7 to 25 V T_j = 25 °C V_i = 8 to 12 V T_j = 25 °C		3 1	100 50	mV mV
ΔV_o*	Load Regulation	I_o = 5 to 1500 mA T_j = 25 °C I_o = 250 to 750 mA T_j = 25 °C			100 50	mV mV
I_d	Quiescent Current	T_j = 25 °C			8	mA
ΔI_d	Quiescent Current Change	I_o = 5 to 1000 mA			0.5	mA
ΔI_d	Quiescent Current Change	V_i = 7 to 25 V			0.8	mA
$\frac{\Delta V_o}{\Delta T}$	Output Voltage Drift	I_o = 5 mA		-1.1		mV/°C
eN	Output Noise Voltage	B = 10Hz to 100KHz T_j = 25 °C		40		µV
SVR	Supply Voltage Rejection	V_i = 8 to 18 V f = 120 Hz	62			dB
V_d	Dropout Voltage	I_o = 1 A T_j = 25 °C		2		V
R_o	Output Resistance	f = 1 KHz		17		mΩ
I_{sc}	Short Circuit Current	V_i = 35 V T_j = 25 °C		750		mA
I_{scp}	Short Circuit Peak Current	T_j = 25 °C		2.2		A

ELECTRICAL CHARACTERISTICS FOR L7852C (refer to the test circuits, T_j = 0 to 125 °C, V_i = 10V, I_o = 500 mA, C_i = 0.33 µF, C_o = 0.1 µF unless otherwise specified)

Symbol	Parameter	Test Conditions	Min.	Typ.	Max.	Unit
V_o	Output Voltage	T_j = 25 °C	5.0	5.2	5.4	V
V_o	Output Voltage	I_o = 5 mA to 1 A $P_o \leq$ 15 W V_i = 8 to 20 V	4.95	5.2	5.45	V
ΔV_o*	Line Regulation	V_i = 7 to 25 V T_j = 25 °C V_i = 8 to 12 V T_j = 25 °C		3 1	105 52	mV mV
ΔV_o*	Load Regulation	I_o = 5 to 1500 mA T_j = 25 °C I_o = 250 to 750 mA T_j = 25 °C			105 52	mV mV
I_d	Quiescent Current	T_j = 25 °C			8	mA
ΔI_d	Quiescent Current Change	I_o = 5 to 1000 mA			0.5	mA
ΔI_d	Quiescent Current Change	V_i = 7 to 25 V			1.3	mA
$\frac{\Delta V_o}{\Delta T}$	Output Voltage Drift	I_o = 5 mA		-1.0		mV/°C
eN	Output Noise Voltage	B = 10Hz to 100KHz T_j = 25 °C		42		µV
SVR	Supply Voltage Rejection	V_i = 8 to 18 V f = 120 Hz	61			dB
V_d	Dropout Voltage	I_o = 1 A T_j = 25 °C		2		V
R_o	Output Resistance	f = 1 KHz		17		mΩ
I_{sc}	Short Circuit Current	V_i = 35 V T_j = 25 °C		750		mA
I_{scp}	Short Circuit Peak Current	T_j = 25 °C		2.2		A

* Load and line regulation are specified at constant junction temperature. Changes in V_o due to heating effects must be taken into account separately. Pulce testing with low duty cycle is used.

58

ELECTRICAL CHARACTERISTICS FOR L7806C (refer to the test circuits, T_j = 0 to 125 °C, V_i = 11V, I_o = 500 mA, C_i = 0.33 µF, C_o = 0.1 µF unless otherwise specified)

Symbol	Parameter	Test Conditions	Min.	Typ.	Max.	Unit
V_o	Output Voltage	T_j = 25 °C	5.75	6	6.25	V
V_o	Output Voltage	I_o = 5 mA to 1 A $P_o \le$ 15 W V_i = 8 to 21 V	5.7	6	6.3	V
ΔV_o*	Line Regulation	V_i = 8 to 25 V T_j = 25 °C V_i = 9 to 13 V T_j = 25 °C			120 60	mV mV
ΔV_o*	Load Regulation	I_o = 5 to 1500 mA T_j = 25 °C I_o = 250 to 750 mA T_j = 25 °C			120 60	mV mV
I_d	Quiescent Current	T_j = 25 °C			8	mA
ΔI_d	Quiescent Current Change	I_o = 5 to 1000 mA			0.5	mA
ΔI_d	Quiescent Current Change	V_i = 8 to 25 V			1.3	mA
$\frac{\Delta V_o}{\Delta T}$	Output Voltage Drift	I_o = 5 mA		-0.8		mV/°C
eN	Output Noise Voltage	B = 10Hz to 100KHz T_j = 25 °C		45		µV
SVR	Supply Voltage Rejection	V_i = 9 to 19 V f = 120 Hz	59			dB
V_d	Dropout Voltage	I_o = 1 A T_j = 25 °C		2		V
R_o	Output Resistance	f = 1 KHz		19		mΩ
I_{sc}	Short Circuit Current	V_i = 35 V T_j = 25 °C		550		mA
I_{scp}	Short Circuit Peak Current	T_j = 25 °C		2.2		A

ELECTRICAL CHARACTERISTICS FOR L7808C (refer to the test circuits, T_j = 0 to 125 °C, V_i = 14V, I_o = 500 mA, C_i = 0.33 µF, C_o = 0.1 µF unless otherwise specified)

Symbol	Parameter	Test Conditions	Min.	Typ.	Max.	Unit
V_o	Output Voltage	T_j = 25 °C	7.7	8	8.3	V
V_o	Output Voltage	I_o = 5 mA to 1 A $P_o \le$ 15 W V_i = 10.5 to 25 V	7.6	8	8.4	V
ΔV_o*	Line Regulation	V_i = 10.5 to 25 V T_j = 25 °C V_i = 11 to 17 V T_j = 25 °C			160 80	mV mV
ΔV_o*	Load Regulation	I_o = 5 to 1500 mA T_j = 25 °C I_o = 250 to 750 mA T_j = 25 °C			160 80	mV mV
I_d	Quiescent Current	T_j = 25 °C			8	mA
ΔI_d	Quiescent Current Change	I_o = 5 to 1000 mA			0.5	mA
ΔI_d	Quiescent Current Change	V_i = 10.5 to 25 V			1	mA
$\frac{\Delta V_o}{\Delta T}$	Output Voltage Drift	I_o = 5 mA		-0.8		mV/°C
eN	Output Noise Voltage	B = 10Hz to 100KHz T_j = 25 °C		52		µV
SVR	Supply Voltage Rejection	V_i = 11.5 to 21.5 V f = 120 Hz	56			dB
V_d	Dropout Voltage	I_o = 1 A T_j = 25 °C		2		V
R_o	Output Resistance	f = 1 KHz		16		mΩ
I_{sc}	Short Circuit Current	V_i = 35 V T_j = 25 °C		450		mA
I_{scp}	Short Circuit Peak Current	T_j = 25 °C		2.2		A

* Load and line regulation are specified at constant junction temperature. Changes in V_o due to heating effects must be taken into account separately. Pulse testing with low duty cycle is used.

59

THIS PAGE INTENTIONALLY LEFT BLANK

LIST OF REFERENCES

Askaryan, G., "Hydrodynamic Radiation from the Tracks of Ionizing Particles in Stable Liquid", *Soviet Journal of Atomic Energy*, 3(1957) 921.

Boyd, T., "Resistivity Surveys", [http://kiska.giseis.alaska.edu/input/west/introgeophys/17_resistivity_surveys/]. March 2006.

Gratta, G., Email correspondence between Giorgio Gratta, Stanford University and LT Michael Gruell, Naval Postgraduate School, January 2005.

Learned, J., Adam, S., Gratta G., Berger, T., Buckingham, M., "Acoustic Radiation by Charged Atomic Particles in Liquids: An Analysis", Physical Review, v.21, n. 11, 1979.

Lehtinen, N., and others, "Sensitivity of an Underwater Acoustic Array to Ultra-High Energy Neutrinos", *Astroparticle Physics,* n.17, 2002.

Sulak, L., Armstrong, T., Baranger, H., Bregman M., Levi, M., Mael D., Strait, J., "Experimental Studies of the Acoustic Signature of Proton Beams Traversing Fluid Media", *Instruments and Methods 161 (1979) 203-217.*

Vandenbroucke, J., Gratta, G., Lehtinen N., "Experimental Study of Acoustic Ultra-High-Energy Neutrino Detection", *The Astrophysical Journal,* v. 621, part 1, p. 301-312.

THIS PAGE INTENTIONALLY LEFT BLANK

INITIAL DISTRIBUTION LIST

1. Defense Technical Information Center
    Ft. Belvoir, Virginia

2. Dudley Knox Library
    Naval Postgraduate School
    Monterey, California

3. William Dewey
    Navy Array Technical Support Center
    Norfolk, Virginia

4. Giorgio Gratta
    Stanford University
    Palo Alto, California

5. Naoko Kurahashi
    Stanford University
    Palo Alto, California

6. Richard Larvia
    Naval Undersea Warfare Center Keyport
    Keyport, Washington

7. Dave Goudy
    Naval Undersea Warfare Center Keyport
    Keyport, Washington

8. Samuel Barone
    Naval Postgraduate School
    Monterey, California

9. Alexander Julian
    Naval Postgraduate School
    Monterey, California

10. Don Snyder
    Naval Postgraduate School
    Monterey, California

THIS PAGE INTENTIONALLY LEFT BLANK